The synaptobrevin homologue Snc2p recruits the exocyst to secretory vesicles by binding to Sec6p

David Shen,[1] Hua Yuan,[1] Alex Hutagalung,[1] Avani Verma,[3] Daniel Kümmel,[2] Xudong Wu,[2] Karin Reinisch,[2] James A. McNew,[3] and Peter Novick[1]

[1]Department of Cellular and Molecular Medicine, University of California, San Diego, La Jolla, CA 92093
[2]Department of Cell Biology, Yale University School of Medicine, New Haven, CT 06520
[3]Department of Biochemistry and Cell Biology, Rice University, Houston, TX 77005

A screen for mutations that affect the recruitment of the exocyst to secretory vesicles identified genes encoding clathrin and proteins that associate or colocalize with clathrin at sites of endocytosis. However, no significant colocalization of the exocyst with clathrin was seen, arguing against a direct role in exocyst recruitment. Rather, these components are needed to recycle the exocytic vesicle SNAREs Snc1p and Snc2p from the plasma membrane into new secretory vesicles where they act to recruit the exocyst. We observe a direct interaction between the exocyst subunit Sec6p and the latter half of the SNARE motif of Snc2p. An *snc2* mutation that specifically disrupts this interaction led to exocyst mislocalization and a block in exocytosis in vivo without affecting liposome fusion in vitro. Overexpression of Sec4p partially suppressed the exocyst localization defects of mutations in clathrin and clathrin-associated components. We propose that the exocyst is recruited to secretory vesicles by the combinatorial signals of Sec4-GTP and the Snc proteins. This could help to confer both specificity and directionality to vesicular traffic.

Introduction

Vesicular traffic between membrane-bound organelles relies on a variety of components that together ensure the selection of appropriate cargo from the donor compartment and faithful transfer of that cargo to the correct target compartment. Nearly all of these components are conserved among eukaryotic organisms (Ferro-Novick and Jahn, 1994). Most are also members of protein families in which different members play analogous roles at different stages of membrane traffic. These include rab GTPases that act as master regulators of membrane traffic (Gurkan et al., 2007; Mizuno-Yamasaki et al., 2012), SNAREs that mediate membrane fusion (Kloepper et al., 2008), and Sec1-munc18 (SM) proteins implicated in both SNARE complex assembly and in coupling SNARE assembly to efficient membrane fusion (Carr and Rizo, 2010). In addition to these components, it has recently become clear that four of the vesicle tethers that mediate the initial recognition of the target membrane by vesicles at different stages of membrane traffic are structurally related to one another, despite very low levels of sequence similarity. This collection of proteins has been alternatively termed the quatrefoil (Whyte and Munro, 2001) and CATCHR family (Yu and Hughson, 2010) and it includes the exocyst, COG, GARP, and Dsl tethering complexes. These tethers all consist of multiple subunits, each containing several helical bundles, strung in series to form rod-shaped elements (Dong et al., 2005). Although their functions remain incompletely understood, interactions with coat proteins, SNAREs, SNARE regulators, lipids, and GTPases of the rab, rho, ral, and arf families have been documented (Novick and Guo, 2002; Munson and Novick, 2006). One interpretation of these many interactions is that the tethers function as scaffolds, holding together, in the optimal orientation, all of the different components needed for efficient docking and fusion of vesicles with the appropriate target membrane (Yu and Hughson, 2010).

The exocyst was the first member of this family to be identified and characterized. This complex consists of one copy of eight different subunits. Six were identified through genetic analysis of the yeast secretory pathway (Novick et al., 1980). These are Sec3p, Sec5p, Sec6p, Sec8p, Sec10p, and Sec15p. The two remaining subunits, Exo70p and Exo84p, were identified through biochemical analysis of the purified complex

Correspondence to Peter Novick: pnovick@ucsd.edu

The Rockefeller University Press $30.00
J. Cell Biol. Vol. 202 No. 3 509–526
www.jcb.org/cgi/doi/10.1083/jcb.201211148

(TerBush et al., 1996; Guo et al., 1999a). Each of these components is required for the final stage of the yeast secretory pathway in which secretory vesicles are directed to fuse with the plasma membrane at sites defined by the cell polarity establishment machinery. At the start of the cell cycle, vesicles are directed to the prebud site and then, as the cycle progresses, to the tip of the emerging bud. Late in the cell cycle, polarity shifts and vesicles are directed to the neck between the bud and mother cell, facilitating cytokinesis and cell separation (Novick and Brennwald, 1993). While all eight exocyst subunits concentrate at these sites, six of them, Sec5p, Sec6p, Sec8p, Sec10p, Sec15p, and Exo84p, achieve this localization exclusively by riding on secretory vesicles as they are actively transported by the type V myosin, Myo2p, along polarized actin cables (Boyd et al., 2004). The other two subunits, Sec3p and Exo70p, can localize to exocytic sites independent of actin function by directly binding to polarity determinants at the cell cortex (Guo et al., 2001). Actin-independent localization requires the N-terminal domain of Sec3p (Guo et al., 2001) and the third helical bundle of Exo70p (Hutagalung et al., 2009). Although neither of these two domains alone is needed for growth, secretion, or exocyst localization, concurrent loss of both domains is lethal even in the presence of multi-copy suppressors that can bypass a complete deletion of either gene (Hutagalung et al., 2009). Thus, it appears to be absolutely essential that at least one of these two subunits interact with polarity determinants on the target membrane.

To function as a vesicle tether, the exocyst must recognize not only the target membrane, but the vesicle membrane as well. Early evidence indicated that Sec15p functions in response to the vesicle-associated rab, Sec4p, implying an interaction with the vesicle surface (Salminen and Novick, 1989). Expression of Sec15p from the strong, inducible *GAL1* promoter leads to the formation of a cluster of secretory vesicles carrying both Sec4p and the overexpressed Sec15p. By fluorescence microscopy, this is manifest as a bright patch of Sec15p that colocalizes with a patch of Sec4p. Patch formation upon Sec15p overexpression is blocked in a *sec4-8* mutant strain or in a *sec2-41* strain defective in the Sec4p guanine nucleotide exchange factor, Sec2p. These findings prompted our proposal that Sec15p acts in response to the activated form of Sec4p (Salminen and Novick, 1989) to tether vesicles. In the context of Sec15p overexpression, this response leads to the formation of a cluster of secretory vesicles, whereas in the context of normal Sec15p expression the response to activated Sec4 is to tether the vesicle to the plasma membrane. Two-hybrid analysis, chemical cross-linking, and pull-down studies all support a direct interaction between Sec15p and Sec4-GTP (Guo et al., 1999b). Although the Sec4p–Sec15p interaction certainly contributes to the recruitment of the exocyst to the surface of secretory vesicles, it is unlikely to be the only interaction involved as, in a *sec4-8* mutant strain, Sec15p still associates with secretory vesicles, even though those vesicles fail to cluster into a patch (Salminen and Novick, 1989). In the current study, we sought to identify additional interactions between the exocyst and components on the surface of secretory vesicles. Our analysis points to a direct interaction between the exocyst component Sec6p and the redundant exocytic v-SNAREs, Snc1p and Snc2p.

Results

Visual screen for exocyst localization mutants

To identify components required for recruitment of the exocyst to secretory vesicles we performed a directed visual screen based on Sec15p localization. We introduced a plasmid expressing Sec15-GFP from the inducible *GAL1* promoter into 73 strains picked from the yeast deletion library. Based on the presumption that a protein that recruits the exocyst to vesicles must itself be at least partially or transiently associated with those vesicles, we chose strains deleted for genes encoding proteins possibly associated with secretory vesicles, such as coat components, or that have been localized to the bud tip or neck where secretory vesicles concentrate before fusion with the plasma membrane.

After induction of Sec15-GFP expression by growth on galactose medium for 5–8 h, wild-type cells uniformly exhibited a bright fluorescent patch of Sec15-GFP (Fig. 1 A, a) similar to that previously seen by immunofluorescence in cells expressing Sec15p from the *GAL1* promoter (Salminen and Novick, 1989). This patch was typically seen at the tip of small buds or at the neck of large budded cells. In wild-type cells and in most of the mutant strains a patch of Sec15-GFP was observed; however, in eight strains we saw a significant reduction in the fraction of cells exhibiting a fluorescent Sec15-GFP patch (Fig. 1 B). These mutants predominantly exhibited diffuse fluorescence throughout the cytoplasm such as is shown for *chc1Δ* cells (Fig. 1 A, b).

All but one of the affected strains were deleted for either a component of the clathrin coat itself, a component known to associate with a specific class of clathrin-coated vesicles, or a component that colocalizes with clathrin by fluorescence microscopy. These include both *chc1Δ* and *clc1Δ*, the structural genes encoding clathrin heavy chain and light chain, respectively. Clathrin-coated vesicles mediate several different transport events (McNiven and Thompson, 2006). Although clathrin is perhaps best known for its role in the formation of endocytic vesicles at the plasma membrane, the same clathrin subunits also act at the Golgi and endosome to direct traffic of specific cargo proteins between these compartments. Different adaptor complexes allow the same clathrin components to be used in different cellular locations. The AP-1 adaptor complex localizes to the trans-Golgi network and recruits clathrin to nascent vesicles destined for the endosome, whereas the AP-2 and AP180/CALM adaptors localize to the plasma membrane and recruit clathrin to nascent endocytic vesicles, and AP-3 localizes to endosomes. Of all the genes encoding subunits of one of the clathrin adaptor complexes, only deletion of *yap1802*, encoding a homologue of the AP-180/CALM adaptor, and *apm4*, encoding the μ subunit of the AP-2 adaptor complex, showed significant defects in the formation of Sec15-GFP patches (Fig. 1 B). Because we observed a defect with one of the deletions of the four subunits of the AP-2 adaptor complex, but not the other three, we backcrossed the *apm4* mutant and tested three different mutant strains. They exhibited on average only a 12% decrease in Sec15-GFP localization. We therefore did not pursue further analysis of the *apm4* mutant.

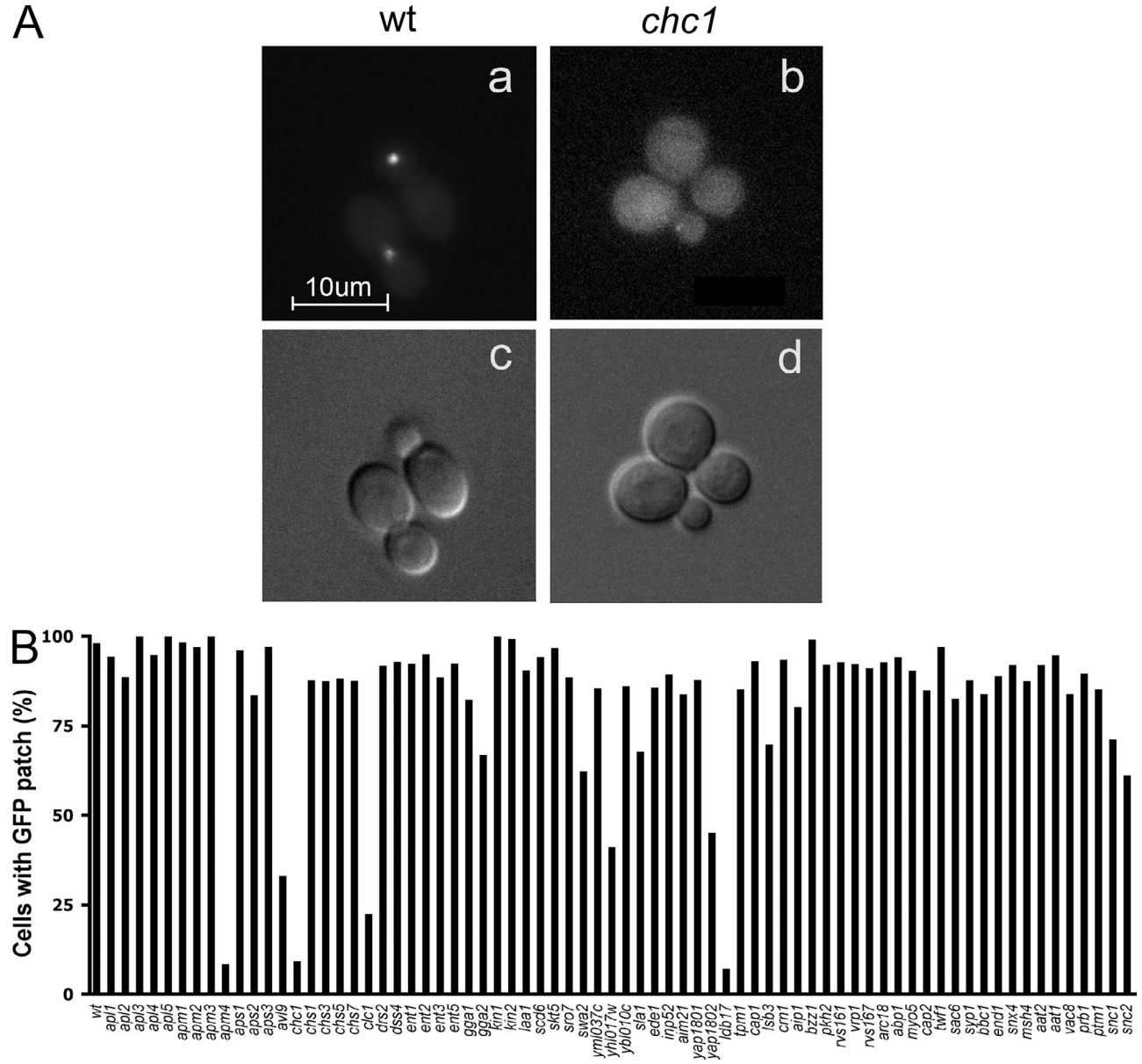

Figure 1. **Visual screening of Sec15p-GFP localization in deletion strains.** Strains were selected from the yeast deletion library and transformed with a *GAL-SEC15*-GFP construct. After 5 h of galactose induction, cells were collected and imaged by fluorescence microscopy. (A) Sec15p-GFP was concentrated at exocytic sites including bud tips and bud necks in WT cells (a), yet appeared diffuse in *chc1Δ* cells (b). The corresponding DIC images are shown in c and d. The appearance of Sec15p-GFP patches was quantified by scoring ~200 cells for each strain (B). Values indicate the percentage of cells showing GFP-labeled patches at the bud tip or bud neck. Bar, 10 μm.

In addition to clathrin and clathrin adaptor proteins, several other clathrin-associated proteins were implicated through our screen, including Ldb17p and Swa2p (Fig. 1 B). Ldb17p was recently shown to colocalize with clathrin at sites of endocytosis on the plasma membrane and to play a role in the selection of specific cargo for internalization (Burston et al., 2009). Swa2p, the yeast homologue of auxillin, acts in conjunction with a chaperone to disassemble clathrin coats for reutilization (Gall et al., 2000; Pishvaee et al., 2000). We also identified the uncharacterized open reading frame YHL017W in our screen. Although no function has been assigned to this gene product to date, it has been shown to colocalize with clathrin-coated vesicles by fluorescence microscopy (Huh et al., 2003). Based on this observation, we have named the gene *CCP1*, for clathrin co-localizing protein 1. In addition to deletions of clathrin and clathrin-associated components, we also identified the *avl9Δ* mutant in our screen. Avl9p is thought to play a role in the formation of a sub-class of secretory vesicles, although its molecular mechanism is not well understood (Harsay and Schekman, 2007).

Because our visual screen used a construct in which Sec15-GFP expression is driven from the strong *GAL1* promoter, a condition that leads to the formation of aberrant vesicle clusters and impaired cell growth, we reexamined the mutants identified in the screen using a Sec15-3xGFP fusion construct, integrated into the *SEC15* locus as the sole copy of

the gene, under normal expression from its own promoter. In general, the mutants identified in our screen exhibited a similar defect in Sec15-3xGFP localization when it was expressed at normal levels (Fig. 2, A and B), although the *ldb17Δ* mutant was not as dramatically affected under these conditions. Importantly, both *chc1Δ* and *clc1Δ* mutants continued to exhibit a profound defect in Sec15-3xGFP localization. Because Yap1802 is redundant in function with Yap1081, we examined a *yap1801Δ yap1802Δ* double mutant, yet found Sec15-3xGFP mislocalization to be similar to that of the *yap1802Δ* single mutant.

Two models for the role of clathrin in exocyst recruitment

We consider below two models to explain the roles of clathrin and clathrin-associated components in Sec15-GFP localization. The simplest model assumes that clathrin is used to form the secretory vesicles that then rely on the exocyst for tethering to the cell cortex and fusion with the plasma membrane. In this model, the exocyst could be recruited to secretory vesicles through a physical interaction with clathrin itself or with one of the clathrin-associated components identified in our screen. Several lines of evidence are broadly consistent with a role for clathrin in the formation of a subset of exocytic vesicles (Gall et al., 2002; Harsay and Schekman, 2007). Furthermore, other tethering complexes have been shown to bind to their respective vesicle coats.

To address this model we assessed the degree of colocalization of Chc1-RFP with Sec15-3xGFP or Sec5-3xGFP (Fig. 3). Chc1-RFP localizes to a collection of cortical puncta, representing sites of endocytosis at the cell surface and to internal puncta, representing Golgi or endosomes. In contrast, Sec15-3xGFP and Sec5-3xGFP localize to the tips of small buds and the necks of large budded cells. Very little colocalization of Chc1-RFP with either exocyst subunit was observed (Fig. 3, A and B). We also tested for colocalization of Chc1-RFP with Sec15-GFP overexpressed from the *GAL1* promoter. Again, very little colocalization was seen.

The lack of colocalization of Sec5p or Sec15p with clathrin led us to consider a second model in which clathrin and its associated components are not required directly for exocyst recruitment, but rather play an indirect role in which they serve to recycle some key secretory vesicle component from the plasma membrane after exocytic fusion. The recycled component would recruit the exocyst only after it had been repackaged into a new secretory vesicle. This model is consistent with the identification of *yap1802Δ* in our screen. Yap1802p is an AP-180/CALM homologue known to play a role in the initial stage of endocytosis at the plasma membrane (Maldonado-Báez et al., 2008).

To explore this model, we considered possible candidates known to be associated with secretory vesicles and internalized from the plasma membrane in a clathrin-dependent fashion. Snc1p and Snc2p (collectively termed Snc1/2p) are redundant synaptobrevin-related v-SNAREs required for the fusion of secretory vesicles with the plasma membrane (Protopopov et al., 1993). Prior studies have established that, after exocytic fusion, they are internalized from the plasma membrane by clathrin-coated vesicles and then recycled through endosomes and the Golgi into new secretory vesicles (Lewis et al., 2000; Burston et al., 2009). Internalization of Snc1/2p from the cell surface requires Yap1801/1802p and Ldb17p in addition to clathrin, consistent with the results of our screen (Burston et al., 2009). Because GFP-Snc1p is normally internalized by endocytosis before it has a chance to diffuse far from sites of exocytosis, it exhibits cortical localization that is strongly polarized to the bud relative to the mother cell. Defects in Snc1p internalization lead to depolarization of the cortical pool (Lewis et al., 2000), whereas defects in recycling back to the cell surface enhance localization to internal puncta, representing endosomes and Golgi. We examined GFP-Snc1p localization in the seven mutants identified in our screen (Fig. S1). Both *clc1Δ* and *chc1Δ* exhibited complete loss of GFP-Snc1p polarization and *yap1802Δ, ldb17Δ* and *ccp1Δ* exhibited partial loss of polarization. A *yap1801Δ* yap1802*Δ* double mutant exhibited more complete mislocalization, as previously reported (Burston et al., 2009). In the *swa2Δ* mutant GFP-Snc1p was predominantly in internal puncta, consistent with its known defect in the uncoating of clathrin-coated vesicles (Gall et al., 2000; Pishvaee et al., 2000). Only *avl9Δ* showed relatively normal GFP-Snc1p localization, suggesting that this mutant may act by an unrelated mechanism.

Snc1/2p function in exocyst localization

One prediction of this model is that loss of Snc1/2p should lead to a loss of Sec15-GFP patch formation. In our screen of the deletion library, we did observe a modest defect in Sec15-GFP localization in both the *snc1Δ* (25% mislocalization) and *snc2Δ* (35% mislocalization) strains (Fig. 1 B). As these genes are functionally redundant, and either one is sufficient for secretory function, the mild loss of localization observed in the single mutants is consistent with this model, but a more stringent test is needed. Because strains deleted for both *SNC1* and *SNC2* are nearly inviable, we used a strain in which the endogenous *SNC1/2* genes are deleted yet growth is maintained by a copy of *SNC1* expressed from the inducible *GAL1* promoter (Protopopov et al., 1993). This strain grows normally in medium containing galactose, but growth begins to slow 4 h after a shift to glucose, a repressing carbon source. The level of Snc proteins is higher than normal during growth on galactose, but falls below normal after 8 h in glucose medium. We introduced fluorescent protein–tagged exocyst alleles into this strain and assessed their localization at 4 and 8 h after the shift. Sec6-2xmCH, Sec8-2xmCH, and Sec15-3xGFP all showed a dramatic loss in polarized localization by 8 h growth in glucose medium (Fig. 4, A and B).

Internalization of Snc1p from the plasma membrane can be specifically blocked by the combination of two mutations: V40A and M43A (corresponding to V39 and M42 in Snc2p; Grote et al., 2000b; Lewis et al., 2000). As a direct test of our proposed requirement for Snc1/2p recycling in exocyst recruitment, we examined Sec15-GFP and Sec6-GFP localization in strains deleted for *SNC1* and expressing either wild-type Snc2p or Snc2-V39A, M42A (Fig. 4, C and D). Localization of both exocyst components was strongly affected in the *snc1Δ snc2-V39M42A* mutant. Broadly dispersed cortical localization was seen rather than the highly polarized pattern typical of wild-type cells. Thus, with respect to exocyst localization, specifically

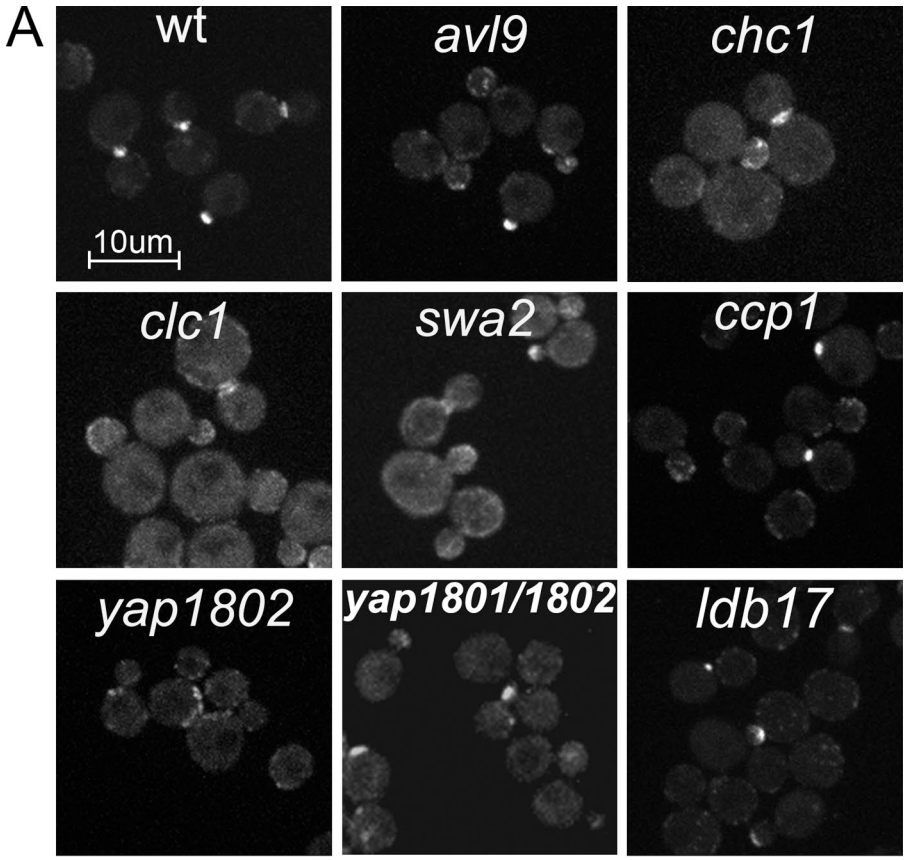

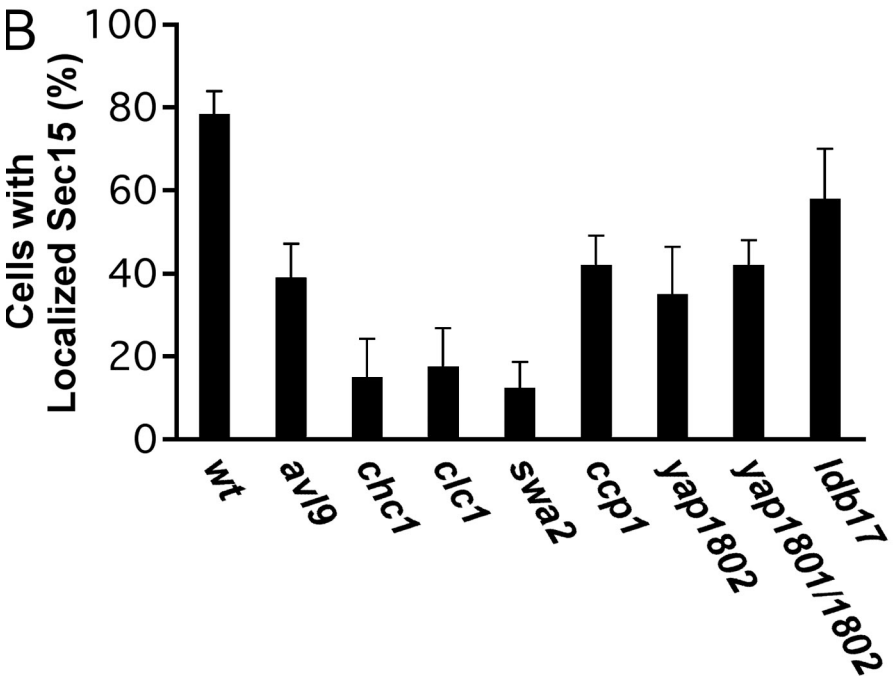

Figure 2. **Localization of Sec15-3xGFP in selected strains.** Sec15p-3xGFP was expressed at normal levels from the endogenous *SEC15* promoter in the seven strains selected from the screen and a *yap1801 yap1802* double mutant. The localization of Sec15p-3xGFP in wild type (wt) or cells carrying the indicated deletions is shown (A). Bar, 10 μm. The localization of Sec15p-3xGFP was quantified (B). Data represent mean ± SD from at least three independent experiments.

blocking Snc2p internalization largely recapitulates the loss of clathrin function.

Interaction of the exocyst with Snc proteins

The postulated recruitment of the exocyst by the Snc1/2 proteins predicts a physical interaction, either direct or indirect, between Snc1/2p and the exocyst. To test this prediction we fused the cytosolic domain of Snc2p to GST and used the purified and immobilized protein to test for binding of the exocyst complex from yeast lysates. We prepared lysates from eight different yeast strains, each expressing a different 13xmyc-tagged exocyst subunit from its own promoter as the sole copy of the gene. As controls we used beads carrying GST, GST-Sec22p

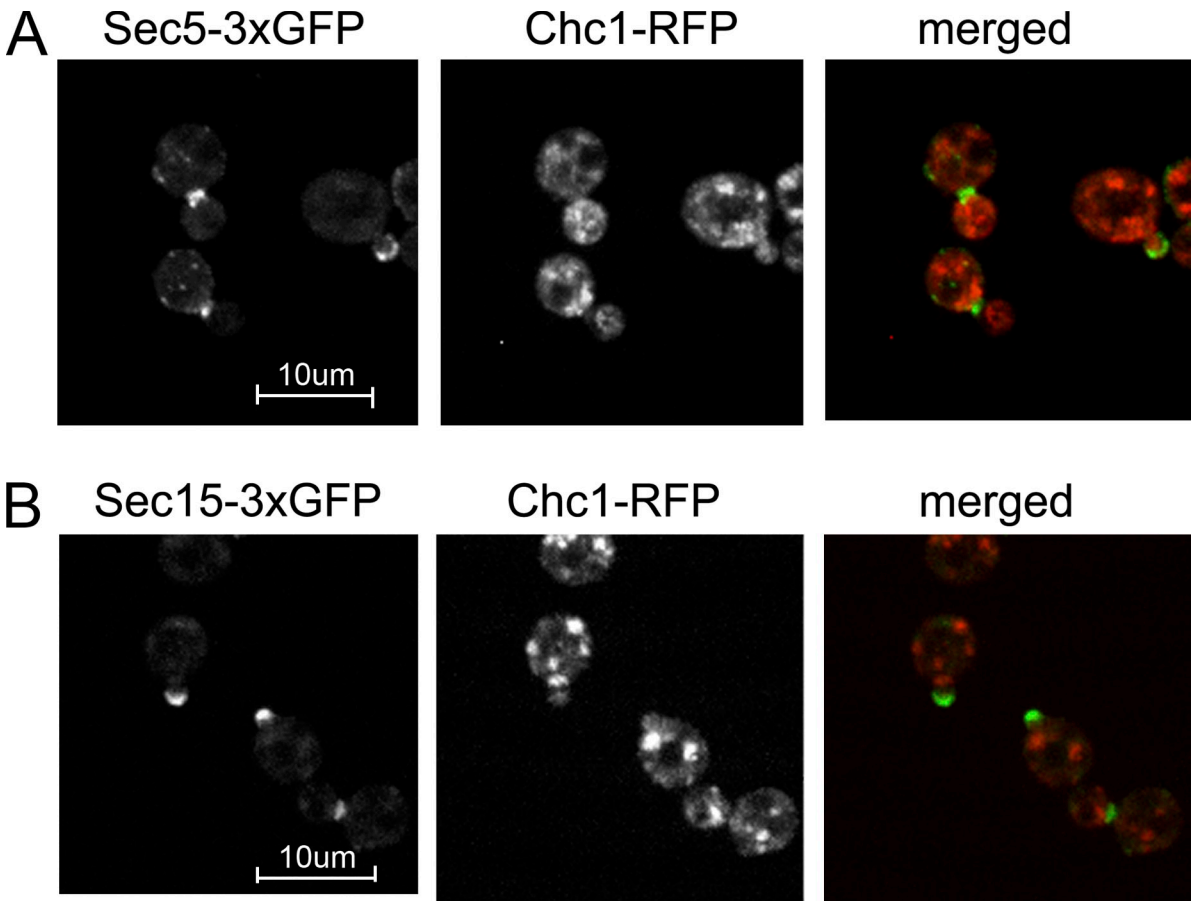

Figure 3. **Localization of Chc1p and exocyst subunits.** Cells coexpressing Chc1p-RFP and (A) Sec5p-3xGFP (NY2983) or (B) Sec15p-3xGFP (NY2984) were grown in selection medium to OD_{600} 0.5 and imaged. Bar, 10 µm.

(a v-SNARE that acts in ER–Golgi transport), and GST-Sso2p (a t-SNARE acting in exocytosis). With six of the lysates we observed significantly more binding of the tagged exocyst subunit to GST-Snc2p than to GST, GST-Sec22p, or GST-Sso2p (Fig. 5 A), suggesting that the largely assembled exocyst complex can specifically bind to Snc2p. Lower specific binding of Sec10p-13xmyc or Sec15p-13xmyc was observed, suggesting that either these tags interfere with binding to Snc2p or that a sub-complex lacking these subunits preferentially binds.

To determine if the observed binding of the exocyst to GST-Snc2p is direct or indirect and to identify the subunit responsible for the interaction we tested individual recombinant exocyst subunits purified from *Escherichia coli* for binding to GST-Snc2p. Of the six exocyst subunits observed to bind from yeast lysates, three can be readily produced in bacteria and purified in large amounts, Sec6p, Exo70p, and Exo84p. Of these, only Sec6p showed efficient binding to GST-Snc2p (Fig. S2).

SNAREs can be characterized by the presence of either a glutamine (Q-SNARE) or arginine (R-SNARE) at the "zero" position at the center of the SNARE four-helix bundle (Fasshauer et al., 1998; Sutton et al., 1998). Assembled SNARE complexes typically contain one R-SNARE and three Q SNARE domains, Qa, Qb, and Qc. By this characterization, Snc1p and Snc2p are R-SNAREs. We tested for binding of Sec6p to all of the other R-SNAREs of yeast, Sec22p, Ykt6p, and Nyv1p, as well as to Sso1p and Sso2p, the redundant syntaxin homologues that serve as Qa-SNARES in exocytic fusion. No interaction was seen with any of these constructs except for very weak binding to GST-Nyv1p (Fig. S2). Using a range of GST-Snc2p concentrations in equilibrium binding reactions we determined that the binding of Sec6p is saturable with a K_d of ~13 µM (Fig. 5 B). Because Snc1p is very similar in sequence and is functionally redundant with Snc2p in vivo, we also tested the interaction of Snc1p with Sec6p. GST-Snc1p also bound Sec6p, although the interaction appeared to be of somewhat lower affinity than the Snc2p–Sec6p interaction (Fig. S3).

To explore the evolutionary conservation of the Sec6p–Snc2p interaction we expressed the human Sec6 homologue, Exoc3, in Hela cells and mixed a cell lysate with lysates of bacteria expressing GST, GST-VAMP3, or GST-VAMP4. After pull-down of the GST constructs, we observed binding of Exoc3 to VAMP3, the vSNARE of the constitutive secretory pathway, but not to its close relative, VAMP4, or to GST (Fig. 5 C).

Defining the binding sites

To define the region of Sec6p that binds to Snc2p we expressed and purified several truncated constructs. Full-length Sec6p bound to Snc2p, yet deletion of 100, 291, or 410 residues from the N terminus prevented binding (Fig. 6 A). This result demonstrates that the N-terminal 1–100 region of Sec6p is necessary

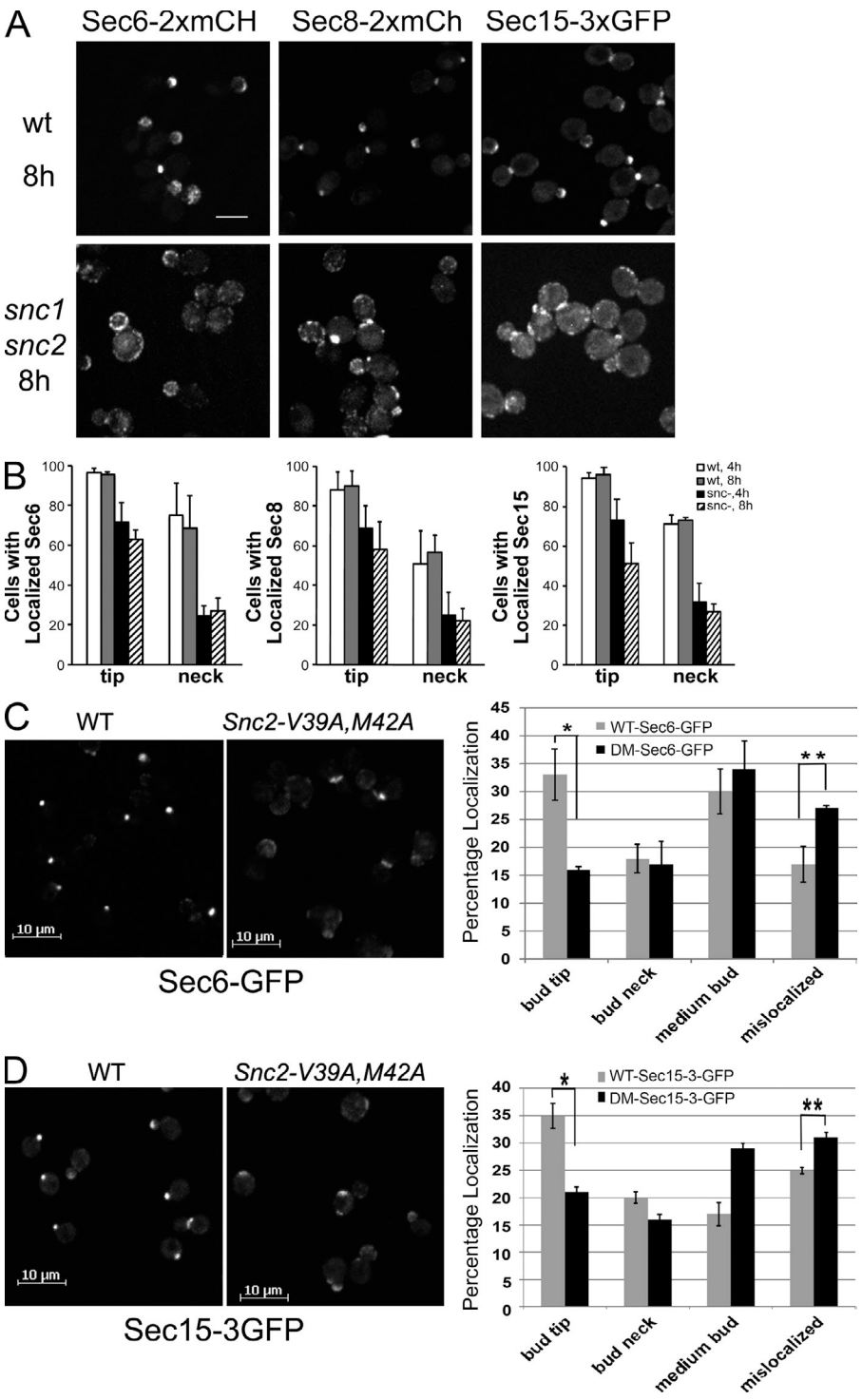

Figure 4. **Snc depletion or blocking its internalization leads to exocyst mislocalization.** (A and B) WT (NY2977, NY2978, and NY2979) and *snc1Δ snc2Δ Gal-SNC1* cells (NY2980, NY2981, and NY2982) expressing Sec6p-2xmCherry, Sec8p-2xmCherry, or Sec15p-3xGFP, respectively, were grown in selection medium containing 4% galactose overnight at 25°C and then switched to selection medium containing 2% glucose at 30°C to block Snc1p expression. The localization of Sec6-2xmCherry, Sec8-2xmCherry, and Sec15-3xGFP was examined (A) and quantified (B) after 4 h and 8 h in glucose medium. Values represent the percentage of cells showing a fluorescent patch at the bud tip or bud neck. At least 100 cells were scored for each condition. Data represent mean ± SD from at least three independent experiments. Bar, 5 μm. (C and D) *snc1Δ SNC2* (NY2986, NY2987) and *snc1Δ snc2-V39A, M42A* (NY2991, NY2992) mutant cells expressing Sec6-GFP (C) or Sec15-3xGFP (D) were grown to early log phase in SD medium at 25°C, and the cells were collected and directly examined by fluorescence microscopy (left). The percentage of cells with fluorescent protein concentrated at prebud site and small bud tip, mother-bud neck, spread over the entire medium bud cortex, or mislocalized (defused over the whole cell cytosol) was quantified (right) for wild type (WT) or the *snc1Δ snc2-V39A, M42A* double mutant (DM). Error bars represent SD. For three separate experiments, $n \approx 400$ cells per count for both wild-type and mutant cells. (C) *, $P < 0.005$; **, $P < 0.01$. (D) *, $P < 0.001$; **, $P < 0.02$, Student's *t* test.

for the interaction with Snc2p. The N-terminal half of Sec6p cannot be produced alone as a soluble protein in *E. coli*; however, when coexpressed with a portion (aa 1–236) of its nearest neighbor in the exocyst complex, Sec8p, a soluble complex containing either Sec6p (1–292) or Sec6p (1–411) can be expressed and purified. The complex containing Sec6p (1–411) and Sec8p (1–236) bound to GST-Snc2p as efficiently as full-length Sec6p, whereas the complex containing Sec6p (1–292) and Sec8p (1–236) showed very little binding (Fig. 6 A). The Sec8p fragment was also detected in the precipitate with Sec6p (1–411). Taken together, these results imply that Snc2p binding requires both the region from aa 1–100 as well as the region from aa 292–411 of Sec6p. Furthermore, our results indicate that the interaction is not blocked by the interaction of Sec8p with Sec6p, a conclusion that is also consistent with the precipitation of at least six of the eight exocyst subunits, including Sec8p, from yeast lysates by GST-Snc2p (Fig. 5 A).

To define the region of Snc2p that is involved in binding to Sec6p, we expressed various Snc2 truncations fused to GST and tested for Sec6p binding. Upstream of the SNARE motif is

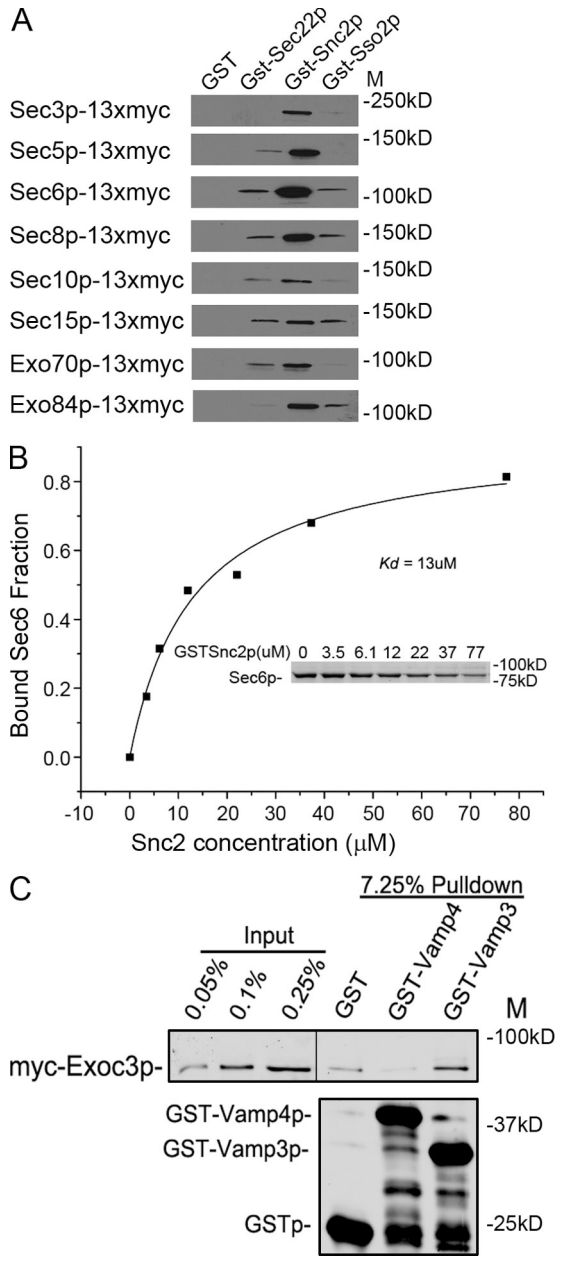

Figure 5. **The exocyst binds to Snc2p.** (A) Lysates were prepared from eight different yeast strains, each expressing, as the sole copy of the gene, a different exocyst subunit fused at the C terminus to a 13xmyc tag. The lysates were incubated with recombinant GST or GST fused to Sec22p, Snc2p, or Sso2p. The amount of GST-tagged protein was assessed by SDS-PAGE and Coomassie staining, using BSA as a standard. Based on this analysis, ~3 µg was added to each binding reaction. Glutathione beads were added and washed and the bound proteins analyzed by immunoblot using anti-myc antibody. (B) The K_d of the Snc2p–Sec6p interaction was determined to be 13 ± 6 µM by a quantitative GST pull-down assay. 0–77 µM GST-Snc2p bound to glutathione beads was incubated with 0.4 µM Sec6p. After pelleting the beads, the unbound fraction of Sec6p was determined by scanning a Coomassie-stained gel of the supernatant (inset). The data shown are from a representative experiment of five independent repetitions. The K_d was calculated using Origin software. (C) Lysates of bacteria expressing GST, GST-Vamp4p, and GST-Vamp3p (0.2 µM final concentration) were mixed with 1 ml lysates of HeLa cells (transfected with plasmid pNB1462) expressing myc-Exoc3 from a 100-mm dish culture, and incubated at 4°C for 2 h. Glutathione beads (10 µl) were added and incubated for another hour. The beads were pelleted and washed three times with binding buffer before SDS-PAGE and Western blot analysis with anti-myc antibody. The black line in the top panel indicates where intervening lanes have been removed for presentation purposes.

a short region (aa 1–28) that proved to be dispensable for binding to Sec6p (Fig. 6 B). The region upstream of the arginine (R52) at the 0 layer at the center of the SNARE motif was also entirely dispensable for Sec6p binding and, on its own, exhibited no detectable affinity for Sec6p, whereas the region between the 0 layer and the transmembrane domain (aa 53–92) binds to Sec6p with an affinity (K_d = 18 µM) comparable to that of full-length Snc2p (K_d = 13 µM; Fig. 6 B). Thus, Sec6p binds to the second half of the SNARE motif.

To further define the binding site within this region we mutated three different charged clusters to either alanines or to residues of the opposite charge. We selected residues that are not directly involved in interactions with the other components of the exocytic SNARE complex (Fig. 7 A). The E51A E54A (M5), E51R E54R (M6), E60A D61A D64A (M3), and E60K D61R D64R (M4) mutations did not significantly affect binding to Sec6. However, both R75A R79A K82A (M1) and R75E R79E K82E (M2) strongly inhibited binding to Sec6p (Fig. 7 B). These results suggest that Sec6p binds to a fairly small region close to the end of the SNARE motif of Snc2p, adjacent to its transmembrane domain. We next made six different mutations in which each of these three charged residues (R75, R79, and K82) were changed singly to either alanine or to glutamate, a residue of the opposite charge (Fig. S4). R75A reduced binding, whereas R75E blocked binding more effectively. Both R79A and R79E were effective in blocking binding. K82A had little effect on binding, whereas K82E strongly blocked binding. Thus, each of these three residues is important for binding, with R79 being somewhat more sensitive to alteration than the other two.

Although the structure of the assembled SNARE complex predicts that the M2 mutations would not affect SNARE assembly, we tested the Snc2-M2 mutant in a liposome fusion assay (Scott et al., 2000) to confirm that its critical fusion functions, which would include its ability to assemble into a SNARE complex, had not been compromised. Liposomes containing either Snc2p or the Snc2-M2p mutant were mixed with liposomes containing the tSNAREs, GST-Sec9c and His6-Sso1p. Lipid mixing, indicative of liposome fusion, was assayed by an NBD fluorescence-dequenching assay. At low protein levels there was no significant difference in the rate of fusion of Snc2-M2 liposomes relative to the wild-type control, and only a small decrease in the rate of fusion was observed at high protein levels (Fig. 7, C and D).

Because the Sec6p binding site is very close to the transmembrane domain of Snc2p, we tested the ability of Sec6p to bind to Snc2p reconstituted into liposomes. Using liposomes containing no Snc2p, full-length Snc2p, or the Snc2-M2p mutant we found that Sec6p can bind specifically to Snc2p liposomes, with at least a twofold reduction in binding to the Snc2-M2p mutant (Fig. 7, F and G). Therefore, the N-terminal region of Sec6p can bind to the membrane-proximal portion of the Snc2p SNARE motif even when Snc2p is anchored in a membrane.

Phenotype of the M2 mutant

The *snc2-M2* mutations were introduced into the genome at the *SNC2* locus of a *snc1Δ* yeast strain and the mutant protein was found to be expressed at a level similar to that of wild-type Snc2p (Fig. 8 D). The *snc1Δ snc2-M2* strain was viable, but

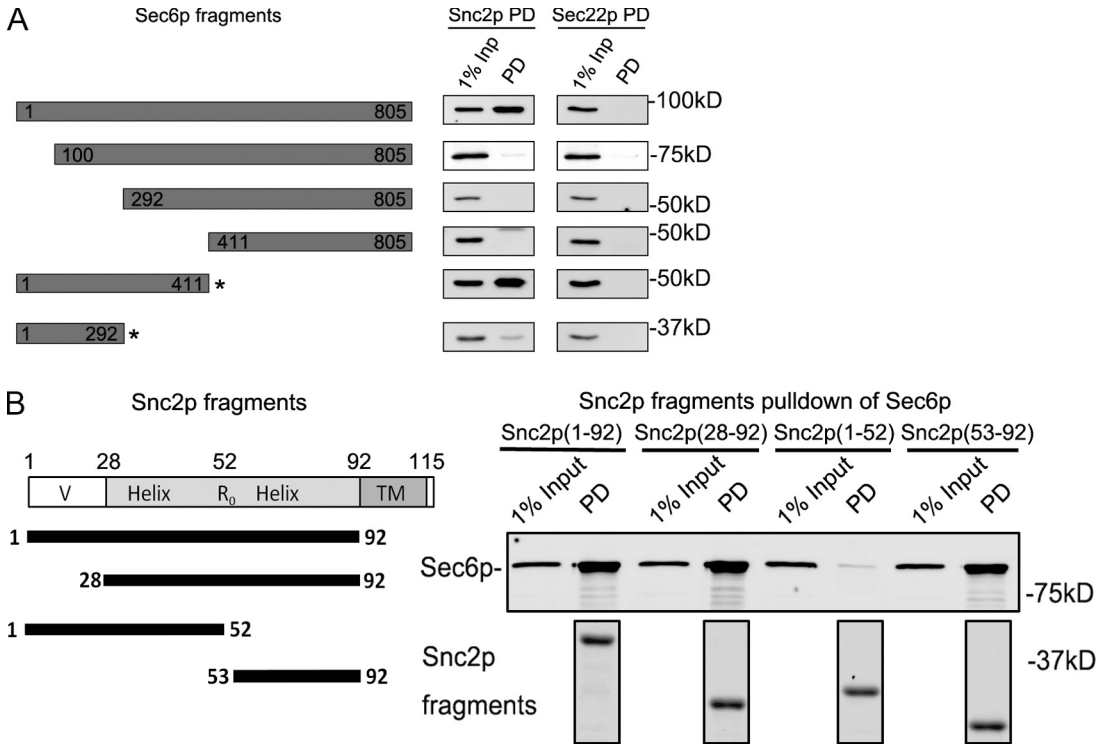

Figure 6. **The N terminus of Sec6p binds to the end of the Snc2p SNARE domain.** (A) Full-length or truncated regions of Sec6p were expressed in bacteria as 6xHis-tagged constructs. The 1–411 and 1–292 fragments (indicated by asterisks) of Sec6p were coexpressed with a fragment of Sec8p (1–236) that binds to them and helps to maintain their solubility. The purified Sec6p fragments or Sec6p–Sec8p complexes (50 nM final concentration) were mixed with Snc2p-GST or Sec22p-GST (50 nM final concentration) in a 1-ml binding assay. The bound proteins were recovered on glutathione beads and analyzed by immunoblot analysis. The region from 1–411 of Sec6p is sufficient for Snc2p binding, whereas both the regions from 1–100 and 292–411 are required. (B) Fragments of Snc2p fused to GST were expressed in bacteria, purified, and mixed at 80 nM (final concentration) with 50 nM (final concentration) His-tagged Sec6p in a 1-ml binding assay. After precipitation of the GST-tagged constructs with glutathione beads (shown in the bottom panel by Coomassie staining of a gel in which intervening lanes have been removed for presentation purposes), the recovery of Sec6p was determined by immunoblot. The region from 53–92 of Snc2p is both necessary and sufficient for Sec6p binding, whereas the N-terminal 1–52 fragment shows no detectable binding. Relevant lanes from the corresponding Coomassie gel are shown in the bottom panel.

exhibited growth defects at both high and low temperatures in comparison to the *snc1Δ SNC2* control (Fig. 8 A). Sec6-GFP and Sec15-3xGFP constructs were introduced into these strains. Although both tagged subunits continued to display a polarized localization in the *snc1Δ snc2-M2* strain, a higher fraction of the cells showed punctate labeling of the entire bud cortex rather than the highly focused localization to the bud tip or mother-bud neck typical of the *snc1Δ SNC2* control (Fig. 8, B and C). The *snc1Δ snc2-M2* mutant cells were also larger than the control cells and were often misshapen, consistent with a defect in the spatial regulation of cell surface assembly.

The function of the secretory machinery can be assessed by measuring the efficiency of invertase secretion after a shift from repressing medium to derepressing medium. The *snc1Δ SNC2* control strain secretes more than 90% of the invertase synthesized during a 1-h period of invertase derepression, whereas the *snc1Δ snc2-M2* mutant secretes only ∼50%, indicating a substantial defect in the secretory machinery (Fig. 8 E).

Secretory vesicles normally fuse with the plasma membrane within a minute of their formation. Even a partial block in fusion therefore leads to a rapid accumulation of vesicles. Thin-section electron microscopy demonstrated an obvious accumulation of secretory vesicles in the *snc1Δ snc2-M2* mutant cells relative to the control (Fig. 8 F).

Interaction of Sec6p with Snc2p and Sec9p

A prior study found that Sec6p interacts with the Qbc exocytic t-SNARE, Sec9p, and that this interaction requires the region of Sec6 from aa 1–300 (Sivaram et al., 2005). This interaction has a significantly higher affinity (K_d = 0.5–1 μM) than the interaction of Snc2p with Sec6p (K_d = 13 μM). Because both Snc2p and Sec9p require the N-terminal region of Sec6p for binding, we sought to determine if Sec6p can bind to both proteins at the same time or if the binding is competitive. We mixed 65 nM His-tagged Sec6p with 2.5 μM GST-Snc2p and 0–1 μM of His-tagged Sec9p. After recovery of GST-Snc2p on glutathione beads, we found no significant effect of up to 1 μM Sec9p on the binding of Sec6p to Snc2p (Fig. 9). Furthermore, Sec9p was found to associate with GST-Snc2p in the presence of Sec6p. This suggests that Sec9p and Snc2p have nonoverlapping binding sites on Sec6p and that the three proteins can form a ternary complex.

Snc and Sec4, parallel signals for exocyst recruitment

Our prior studies had suggested a role for Sec4-GTP in exocyst recruitment. Activation of Sec4p is required for patch formation upon Sec15p overexpression (Salminen and Novick, 1989) and

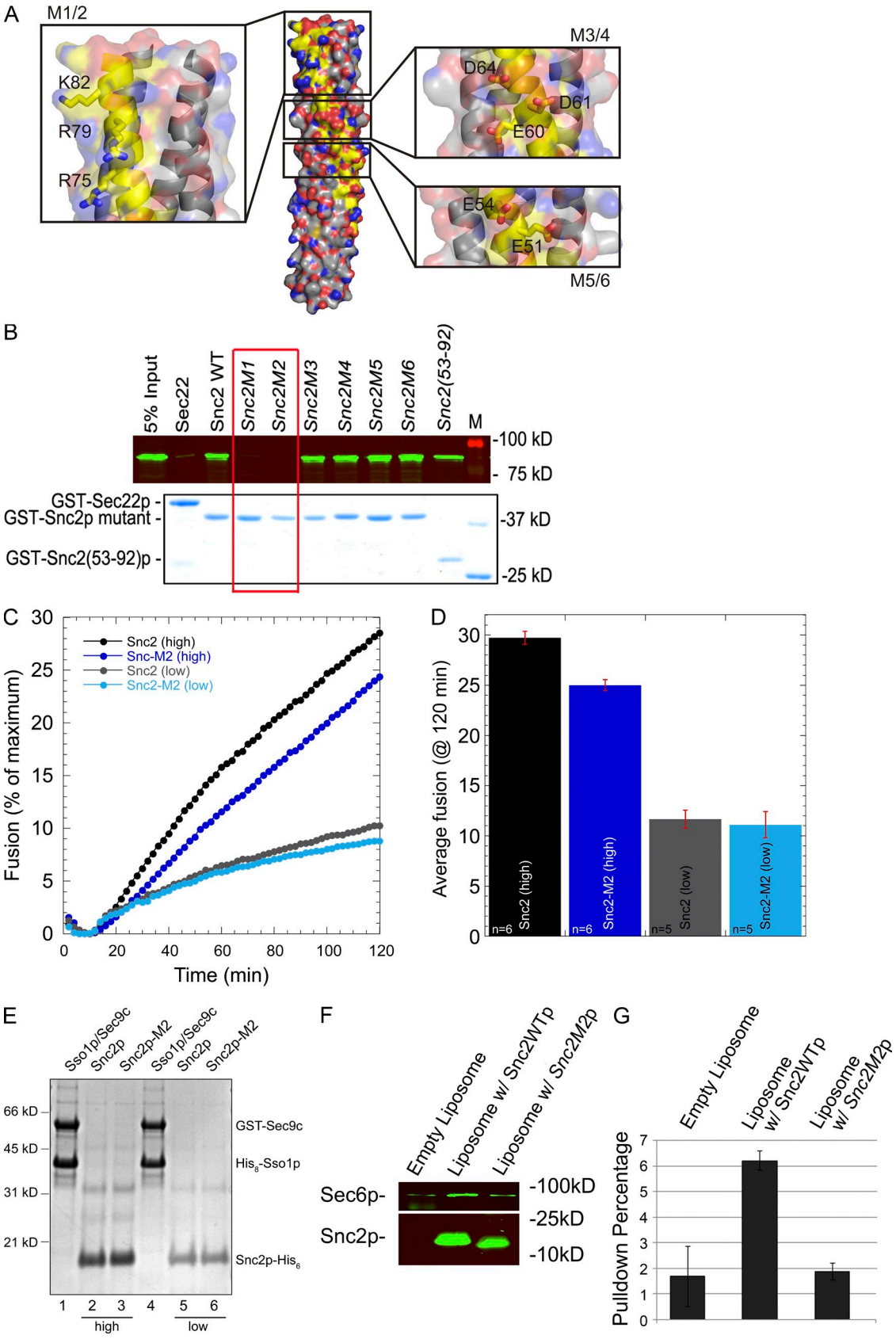

Figure 7. **A positively charged patch at the end of the Snc2p SNARE domain is needed for Sec6p binding, but not liposome fusion.** (A) The structure of the Snc2p–Ssop–Sec9p SNARE complex is shown with the Snc2p backbone highlighted in yellow and the three charged patches on the surface of Snc2p expanded in insets with side chains shown. Images were generated by PyMol using coordinates of 3B5N from the PDB provided by Strop et al. (2008). Snc1p in the original structure was replaced with Snc2p. (B) Binding of Sec6p to Snc2p mutants. His-tagged Sec6p (80 nM final concentration)

Sec15p binds to Sec4p in its GTP-bound conformation (Guo et al., 1999b). Therefore, we considered the possibility that the Snc–Sec6p interaction acts in parallel with the Sec4–Sec15 interaction to promote exocyst recruitment. The exocyst could thereby act as a coincidence detector, requiring the combined vSNARE and rab signals for effective recruitment. A prediction of this proposal is that increasing one signal might compensate for partial loss of the other. We therefore introduced *SEC4* on a high copy number plasmid into the various deletion mutants that affect exocyst localization and observed the effect on Sec15-GFP localization. Overexpression of Sec4p led to a substantial restoration of Sec15-GFP localization in all of these mutants, with the sole exception of *swa2Δ* (Fig. 10). For unknown reasons, overexpression of Sec4p in the *swa2Δ* mutant caused a severe growth defect, which may interfere with any potential restoration of Sec15-GFP localization.

Discussion

We have established here a direct interaction between the Sec6p subunit of the exocyst complex and the secretory vesicle v-SNARE, Snc2p, and have shown that this interaction is critical in vivo for recruitment of the exocyst and for exocytosis. We previously showed that another exocyst subunit, Sec15p, binds to the activated form of the vesicle-associated rab, Sec4p, and proposed that this interaction is needed for recruitment of the exocyst to secretory vesicles (Salminen and Novick, 1989; Guo et al., 1999b). Results we present here suggest that the Snc proteins work in parallel with Sec4-GTP to recruit the exocyst. By binding to both Snc1/2p and Sec4p, each with relatively modest affinity, the exocyst could act as a coincidence detector, associating only with membranes carrying both key ligands. Although Snc1/2p, as a rapidly recycling, integral membrane protein, is necessarily present on both exocytic and endocytic vesicles, Sec4p is only found on the exocytic leg of this circular route and hence the exocyst preferentially associates with secretory vesicles. This asymmetry may help to establish the directionality of vesicle transport. Prior studies have demonstrated interactions of several exocyst subunits with components of the plasma membrane (Guo et al., 2001; He et al., 2007). Together, these findings help to define the molecular links by which the exocyst tethers secretory vesicles to the plasma membrane in preparation for exocytic membrane fusion.

The need to efficiently recycle Snc proteins from the plasma membrane into new secretory vesicles explains the observed requirement for clathrin in exocyst localization. Our screen identified a number of components, in addition to clathrin, that are important for Sec15-GFP localization. Yap1802p is a clathrin adaptor, homologous to the AP180/CALM adaptor proteins of mammalian cells, and has been shown to act at the plasma membrane to internalize Snc1p (Maldonado-Báez et al., 2008; Burston et al., 2009). Aux1–Swa2p is the yeast homologue of auxillin, a protein needed for disassembly of clathrin coats and therefore required for ongoing cycles of clathrin function (Gall et al., 2000; Pishvaee et al., 2000). We also identified Ldb17p, and although this protein is not as well studied, it too colocalizes with clathrin at sites of endocytosis and has been shown to be required for endocytosis of Snc1p (Burston et al., 2009). YHL017W encodes a protein we have named Ccp1 that has been shown to colocalize with clathrin in yeast (Huh et al., 2003), and although nothing more is known regarding its function, we observe a depolarization of cortical GFP-Snc1 in the *ccp1* mutant that suggests a defect in internalization. The one component we identified that may act at a different site is Avl9p. This protein is required for the formation of a subset of secretory vesicles (Harsay and Schekman, 2007). The failure to form these vesicles may result in a substantial reduction in the pool of vesicle-associated exocyst components and hence a loss of Sec15-GFP localization.

Two prior studies in animal cells have noted functional connections between the exocyst and clathrin or its associated adaptors. *Drosophila* oocytes take up large amounts of yolk proteins through clathrin-mediated endocytosis of the yolk receptor, Yolkless. The exocyst subunit Sec5 was found to localize to clathrin-coated pits and vesicles at the plasma membrane of the oocyte (Sommer et al., 2005). Nonetheless, a *sec5* mutation did not disrupt internalization of Yolkless. Rather, in a *sec5* mutant, the receptor was found to accumulate in secretory granules that were blocked in exocytic fusion with the plasma membrane. No physical interaction between the exocyst and clathrin

was mixed with 50 nM (final concentration) of the various Snc2p mutants or with GST-Sec22p as a control. Both *M1 (R75A R79A K82A)* and *M2 (R75E R79E K82E)* show a loss of Sec6p binding activity, whereas *M3 (E60A D61A D64A)*, *M4 (E60K D61R D64R)*, *M5 (E51A E54A)*, and *M6 (E51R E54R)* bind normally. (C) Kinetic fusion assay comparing different donor v-SNARE liposomes containing either wild-type Snc2p or Snc2p-M2 mutant. t-SNARE liposomes containing GST-Sec9c and His6-Sso1p (45 µl) were mixed with 5 µl v-SNARE liposomes and NBD fluorescence was monitored in a fluorescent plate reader for 2 h. Fusion with t-SNAREs (~460 pmol of t-SNARE complex proteins, ~55.8 nmol lipid) and wild-type Snc2p (high, ~136 pmol protein, 4.5 nmol lipid) are shown in black circles, whereas fusion with Snc2p-M2 (high, ~192 pmol protein, 4.6 nmol lipid) are shown in dark blue. Similarly, t-SNARE liposomes with less total protein (~200 pmol of t-SNARE complex proteins, ~28.3 nmol lipid) were fused with wild-type Snc2 liposomes (low, 21 pmol protein, 2.2 nmol lipid, gray circles) or Snc2p-M2 liposomes (low, ~15 pmol protein, 1.3 nmol lipid, light blue circles). Representative traces are shown. (D) Average endpoint fusion. The black and dark blue bar graphs represent fusion with high concentrations of the v-SNARE protein (wild-type and mutant) in the liposomes, whereas gray and light blue bar graphs represent fusion with low concentrations of the v-SNARE proteins (wild type and mutant) in the donor liposomes. The histograms show mean fusion at 120 min and the error bars represent SEM. The number of replicates (*n*) is shown at the base of the histogram. (E) Coomassie blue–stained gel of proteoliposomes on a 10% Bis-Tris NuPAGE Novex gel (Invitrogen). Lanes 1–4 contain 5 µl of proteoliposomes, whereas lanes 5 and 6 (low concentration v-SNAREs) contain 10 µl of proteoliposomes. (F) Sec6p binds to Snc2p reconstituted into liposomes. Empty liposome (0.01 mM lipid) or liposomes containing 0.4 µM Snc2p or Snc2p-M2 were incubated with 0.025 µM His-Sec6 (final concentration) at 4°C for 2 h in 1 ml binding buffer (25 mM Hepes-KOH and 200 mM KCl, pH 7.4, with 0.5 µg/µl BSA). Liposomes were pelleted at 300,000 *g* for 20 min in an ultracentrifuge (Optima TLX; Beckman Coulter) with a TLA 120.2 rotor. The pellet was washed with 1 ml binding buffer and re-pelleted. The pellet was resuspended in 80 µl sample buffer. 10 µl of each sample was resolved by SDS-PAGE and analyzed by Western blot using anti-His (top) and anti-Snc (bottom) antibody. (G) Quantitation of Sec6p binding.

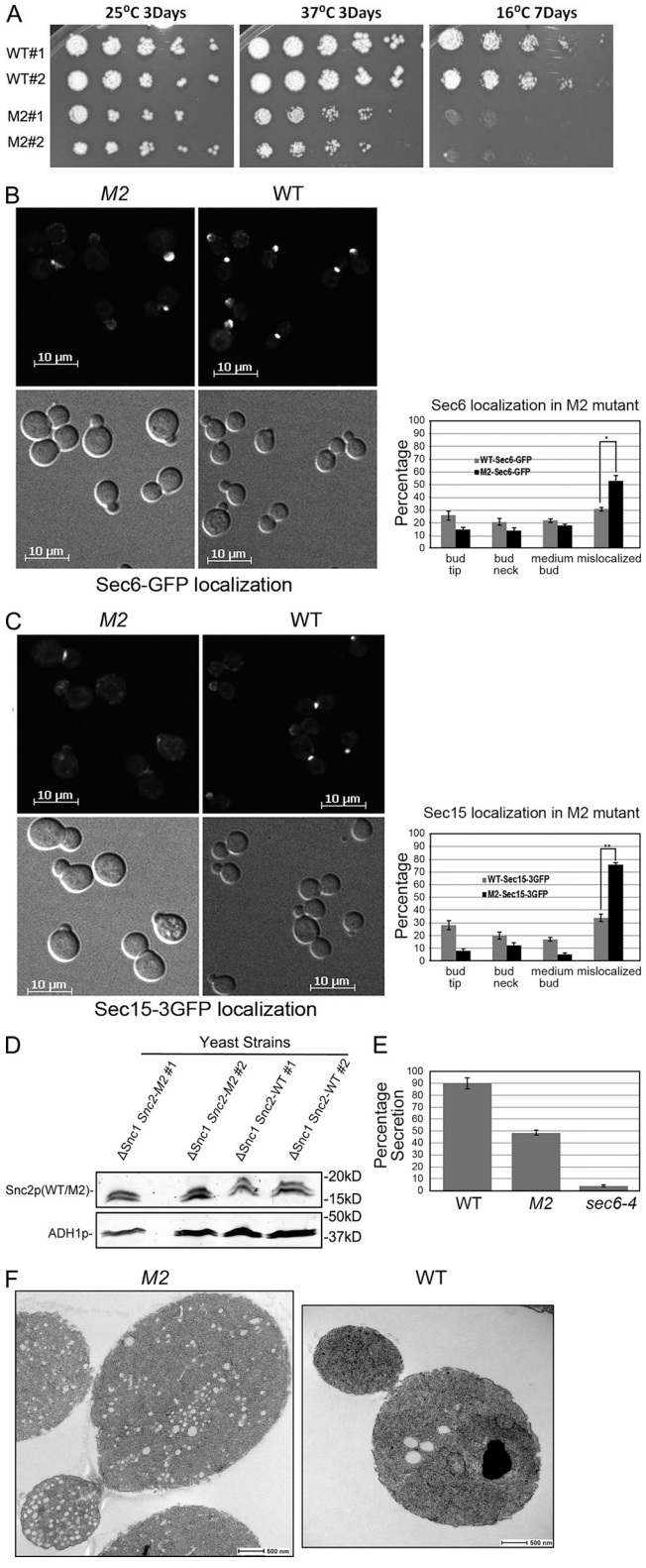

Figure 8. **The *snc2-M2* mutation inhibits growth, localization, and secretion.** (A) Two independent *snc1Δ SNC2* (WT, NY2985) and *snc1Δ snc2-M2* (*M2*, NY2988) yeast strains were serially diluted by fivefold increments, plated and incubated as indicated. The *snc2-M2* mutant shows growth defects at both high and low temperatures. (B) *snc1Δ SNC2* (WT, NY2986) and *snc1Δ snc2-M2* (M2, NY2989) yeast expressing Sec6p-GFP were grown to early log phase in SD medium at 25°C. The cells were collected and directly examined by fluorescence microscopy (left panels). The percentage of cells with Sec6p-GFP at prebud sites and small bud tips, mother-bud necks, spread over the entire medium bud cortex, or mislocalized (defused over the whole cell cytosol) was quantified (right). Error bars represent SD for two independent experiments, $n = 709$ for wild type and $n = 792$ for the *snc2-M2* mutant. *, <0.02, Student's *t* test. (C) *snc1Δ SNC2* (WT, NY2987) and *snc1Δ snc2-M2* (*M2*, NY2990) yeast expressing Sec15p-3xGFP were grown to early log phase in SD medium at 25°C. The cells were collected and directly examined by fluorescence microscopy (left panels). The percentage of cells with Sec15p-3xGFP at prebud sites and small bud tips, mother-bud necks, spread over the entire bud cortex, or mislocalized (defused over the whole cell cytosol) was quantified (right). Error bars represent SD for two independent experiments, $n = 709$ for wild type and $n = 792$ for the *snc2-M2* mutant. **, <0.005, Student's *t* test. (D) Expression of Snc2-M2p is similar to that of Snc2p. (E) Invertase assay. *snc1Δ SNC2* (WT, 2985), *snc1Δ snc2-M2* (*M2,* NY2988), and *sec6-4* (NY17) yeast were grown overnight at 25°C in YP medium containing 5% glucose then transferred to YP medium containing 0.1% glucose and incubated at 37°C for 1 h. The bar graph displays the percentage of invertase synthesized during the 1-h incubation that was delivered to the cell surface. (F) *snc1Δ SNC2* (NY2985, right) *and snc1Δ snc2-M2* (NY2988, left) cells were grown at 25°C in YPD medium and processed for thin section electron microscopy.

or the AP-2 adaptor was observed. These results, like those we report here, are consistent with a model in which the exocyst is recruited by a component that is concentrated in clathrin-coated pits on the plasma membrane and internalized by a clathrin-dependent mechanism. As in yeast, the relevant cargo of the clathrin-coated vesicles may be the v-SNARE required for exocytic fusion. The greatly enhanced level of endocytosis and membrane recycling in oocytes may exaggerate the pool of exocytic v-SNAREs associated with clathrin-coated pits and vesicles. The resulting high concentration of the v-SNARE might bypass the requirement for a coincident rab signal in exocyst recruitment. In this way, the exocyst would be recruited onto endocytic compartments, but still wouldn't function until it recycles with the v-SNARE to an exocytic compartment. Although, in this situation, the exocyst might be recruited to membranes lacking exocytic rabs, activation by an exocytic rab would still be needed to initiate its tethering function.

Polarized epithelial cells rely on the exocyst for export to their basolateral surface. Sorting of cargo by the AP-1 clathrin adaptor occurs in the trans-Golgi network (TGN) and recycling endosomes. The AP-1 complex has two isoforms that differ in their µ subunit: AP-1A, which acts at the TGN, and AP-1B, which acts at the recycling endosome. LLC-PK1 cells, which lack the µ1B subunit, fail to recruit the exocyst to the recycling endosome and are defective in sorting to the basolateral surface (Fölsch et al., 2003). Although expression of µ1B was found to restore exocyst localization in LLC-PK1 cells, no direct interaction of the exocyst with clathrin or the AP-1B adaptor was detected in this study. These results are consistent with a role for clathrin and the AP-1B adaptor in sorting a key component, possibly the exocytic v-SNARE, into vesicles destined for the basolateral surface. The v-SNARE would then serve to recruit the exocyst and thereby prepare the vesicles for tethering and fusion to the basolateral plasma membrane.

Sec6p interacts with a number of different components including itself, other members of the exocyst complex, such as Sec8p, Sec10p, and Exo70p, and other components of the exocytic machinery such as Snc1/2p, Sec9p, and Sec1p (Dong et al.,

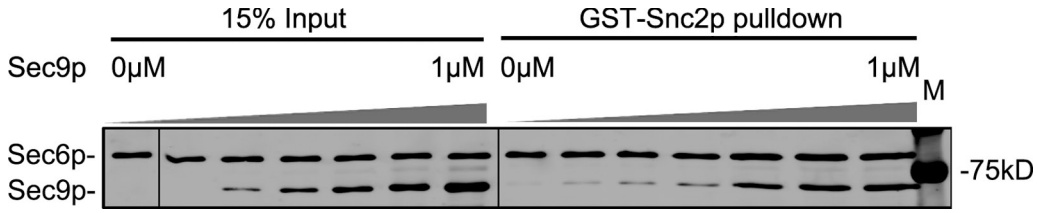

Figure 9. **Sec9p does not interfere with the Snc2p–Sec6p interaction.** GST-Snc2p (2.5 μM final concentration) was incubated with 70 nM (final concentration) His-Sec6p and increasing amounts of His-MBP-Sec9c, as indicated, and then precipitated with glutathione beads. The bead-associated protein was analyzed by SDS PAGE and Coomassie staining. Black lines indicate where lanes have been rearranged for presentation purposes.

2005; Sivaram et al., 2005; Munson and Novick, 2006; Morgera et al., 2012). It will be important to define when in the exocytic reaction and where in the cell each of these interactions occurs, as well as which interactions are mutually compatible and which are not. We have shown here that the interaction of Sec6p and Snc2p is compatible with the interaction of Sec6p and the Qbc-SNARE Sec9p, suggesting a possible role in SNARE complex assembly. Such a role would be fully consistent with the rapid drop in SNARE complex levels after a shift of *sec6*-4 cells to their restrictive temperature (Grote et al., 2000a). Nonetheless, it has been reported that addition of the pure Sec6p homodimer actually slows the formation in vitro of the Sso1p–Sec9p binary tSNARE complex that serves as the rate-limiting intermediate in assembly of the ternary Snc1p–Sso1p–Sec9p complex (Sivaram et al., 2005). We show here that the interaction of Sec6p with Snc2p can occur within the context of a largely assembled exocyst complex. Clearly, more studies will be needed to understand the roles of the other components of the exocyst and other elements of the exocytic machinery in the SNARE assembly reaction. Other, structurally related, tethering complexes have been shown to bind to both the v-SNARE and t-SNAREs that act at the same stage of membrane traffic (Sivaram et al., 2005; Yu and Hughson, 2010). These interactions may serve an important role in linking the transport vesicle, initially through the tether, to the target compartment and in catalyzing the subsequent assembly of the SNARE complex.

Materials and methods

Yeast strains, construction, and media

The strains and plasmids used in this study are listed in Tables 1–5. NY2977 and NY2978 were obtained by transforming plasmids pNB1459 and pNB1460, respectively, into NY438, whereas NY2979 was made by transforming pNB1458 into NY1745. NY2980 and NY2981 were constructed by transforming pNB1459 (pRS305-Sec6-2xmCherry) and pNB1460 (pRS305-Sec8-2xmCherry), respectively, into NY1127. NY2982 was obtained by crossing NY2979 with NY1127. The strains were grown in selection media containing 4% galactose at 25°C. To turn off the inducible *GAL1* promoter, cells were diluted in selection medium containing 2% glucose starting at an OD_{600} of 0.1. At 2-h intervals the growth rate was determined by measuring the OD_{600} and cells were collected for images and immunoblot analysis. Wild-type strains were analyzed under the same conditions. NY2983 and NY2984 were obtained by transforming pNB1304 and pNB1308, respectively into strain EY1669 (Huh et al., 2003). pJM997 (Snc2-M2-His6) was generated by PCR using oligos 93 (NcoI-Snc2 5′-GGCCATGGGTTCATCATCAGTGCCATACG-3′) and 94 (Snc2-XhoI 5′-GAGATATCCTCGAGGCTGAAATGGACGACGATAGG-3′) with PNB1461 (Snc2-M2) as template. The Snc2-M2 PCR product was digested with NcoI and XhoI and ligated into pET28a-based vector (pJM235) digested with the same enzymes. Deletion of both *yap1801* and *1802* was performed by disrupting the *YAP1801* gene in the *yap1802* deletion mutant using a PCR product to replace the ORF of *YAP1801*.

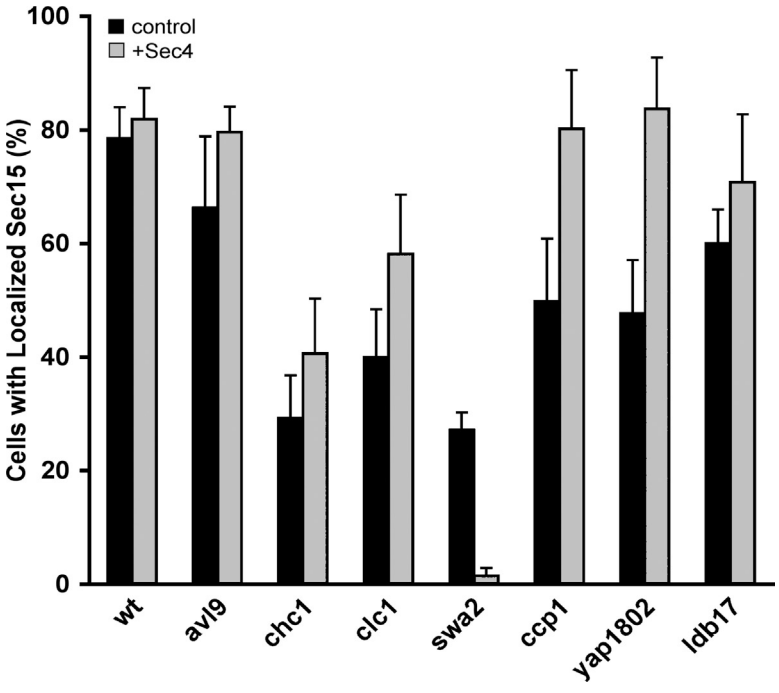

Figure 10. **Overexpression of Sec4p partially restores Sec15p localization.** WT or the indicated deletion mutant strains expressing Sec15-3xGFP were transformed with a 2μ circle-based plasmid overexpressing Sec4p (pNB1457) and examined by fluorescence microscopy. The percentage of cells exhibiting a Sec15p-3xGFP patch at the bud tip or mother-bud neck is shown. Data represent mean ± SD from at least three different experiments.

Table 1. **Deletion strains carrying GAL1-Sec15-GFP**

Strain	Deleted gene	Strain	Deleted gene	Strain	Deleted gene
HY1	*apl1*	HY29	*kin2*	HY57	*myo5*
HY2	*apl2*	HY30	*laa1*	HY58	*cap2*
HY3	*apl3*	HY31	*scd6*	HY59	*twf1*
HY4	*apl4*	HY32	*skt5*	HY60	*sac6*
HY5	*apl5*	HY33	*sro7*	HY61	*syp1*
HY6	*apm1*	HY34	*swa2*	HY62	*bbc1*
HY7	*apm2*	HY35	YML037C	HY63	*end1*
HY8	*apm3*	HY36	*ccp1*	HY64	*snx4*
HY9	*apm4*	HY37	YBL010C	HY65	*msh4*
HY10	*aps1*	HY38	*sla1*	HY66	*aat2*
HY11	*aps2*	HY39	*ede1*	HY67	*aat1*
HY12	*aps3*	HY40	*inp5*	HY68	*vac8*
HY13	*avl9*	HY41	*aim21*	HY69	*prb1*
HY14	*chc1*	HY42	*yap1801*	–	–
HY15	*chs1*	HY43	*yap1802*	–	–
HY16	*chs3*	HY44	*ldb17*	–	–
HY17	*chs5*	HY45	*tpm1*	–	–
HY18	*chs7*	HY46	*cap1*	–	–
HY19	*clc1*	HY47	*lsb3*	–	–
HY20	*drs2*	HY48	*crn1*	–	–
HY21	*dss4*	HY49	*aip1*	–	–
HY22	*ent1*	HY50	*bzz1*	–	–
HY23	*ent2*	HY51	*pkh2*	–	–
HY24	*ent3*	HY52	*rvs161*	HY80	*ptm1*
HY25	*ent5*	HY53	*vrp1*	HY81	*snc1*
HY26	*gga1*	HY54	*rvs167*	HY82	*snc2*
HY27	*gga2*	HY55	*arc18*	–	–
HY28	*kin1*	HY56	*abp1*	–	–

Screening of yeast deletion library

The *Saccharomyces cerevisiae* strain BY4741 (MATa, *his3Δ1, leu2Δ0, met15Δ0, ura3Δ0*) and its derivatives were used in this study (Thermo Fisher Scientific). The 73 strains selected were grown at 25°C in YPD medium supplemented with G418 (200 µg/ml) to OD_{600} ∼1.0 and transformed with pNB1456 (constructed by fusing GFP to Sec15p in pNB300) using the lithium-acetate protocol. After appropriate selection, cells were grown overnight in SC medium containing 2% raffinose at 25°C to reach an absorbance of approximately OD_{600} 1.0 ($Abs_{600\ nm}$), then diluted to OD_{600} 0.1 in SC medium containing 2% raffinose and 2% galactose at 25°C. After 5 h, cells were collected at OD_{600} 0.5–0.8 and Sec15-GFP localization was examined by fluorescence microscopy. To examine the localization of Sec15 expressed at normal levels under its own promoter, the eight strains identified in the initial screen were transformed with the integrating vector pNB1308.

Live-cell fluorescence microscopy and quantitative analysis

Yeast cells were grown at 25°C to early log phase (OD_{600} 0.3–0.6). 500 µl of cells were pelleted and resuspended in growth medium. Fluorescence images were acquired with a 63× oil immersion objective (Plan Apochromat 63×/1.4 oil DIC; Carl Zeiss) on a spinning disc confocal microscopy system (Yokagawa Corporation of America), which included a microscope (Observer Z1; Carl Zeiss) equipped with an electron multiplying CCD camera (QuantEM 512SC; Photometrics). Excitation of GFP or mCherry was achieved using 488-nm argon and 568-nm argon/krypton lasers, respectively. For each sample, a z-stack of 14–18 slices with a 300-nm slice distance was generated. Images were analyzed using AxioVision software 4.8 (Carl Zeiss). Exocyst localization was scored based on localization at the tips of small buds or the necks of large buds. 100–200 cells were examined for each condition and at least three separate experiments were used to calculate the SD.

Protein purification from *E. coli*

GST-Snc2p, GST-Snc2p fragments, His-Sec6p, His-Sec6p fragments, and His-MBP-Sec9ct (416–651 aa) were expressed and purified from corresponding *E. coli* strains. In brief, cells were grown at 37°C to OD_{600} 0.8, then 0.2 mM IPTG (final concentration) was added to induce protein expression and the culture was incubated at 16°C for 12 h with shaking. Cells were harvested by centrifugation for 10 min at 3,500 rpm and resuspended in binding buffer (20 mM Pipes, pH 6.8, 100 mM NaCl, 1% NP-40, 1 mM DTT, and 2 mM PMSF; for His-tagged protein purification no DTT was added) at a cell density of 40 OD_{600} U/ml. Cells were sonicated for 20-s intervals with 20-s breaks for a total of 2 min. Lysates were cleared by centrifugation at 15,000 rpm for 30 min at 4°C. The target protein was purified with glutathione–Sepharose 4B beads (GE Healthcare) for GST fusion proteins or Ni-NTA Agarose beads (QIAGEN) for His-tagged proteins. The His-Sec6 fragments of 1–411 aa (NRB1477) and 1–292 aa (NRB1478) were coexpressed with a Sec8 (1–236 aa) fragment, purified with glutathione beads and cut with PreScission protease (GE Healthcare). The protease is GST tagged and was removed with glutathione beads. The concentration of purified protein was determined by SDS-PAGE with BSA as standard. GST-Sec9c (BB442; Katz et al., 1998), pJM88, pJM81 (McNew et al., 2000), and pJM997 were expressed and purified as described previously (Scott et al., 2003) with the following modifications: cells expressing pJM81 and pJM997 were induced overnight at 20°C with 0.2 mM IPTG, and cells expressing pJM88 were induced for 4 h at 37°C with 0.3 mM IPTG. All his-tagged proteins were purified using an ÄKTAprime low-pressure chromatography system (GE Healthcare) and 1-ml HiTrap HP metal-chelating column (GE Healthcare).

Yeast lysate preparation

50 ml yeast cultures were grown overnight to 1 OD_{600}, harvested by centrifugation at 3,000 rpm for 5 min, and washed once with distilled water and resuspended in 1.4 ml ice-cold binding buffer (20 mM Pipes, pH 6.8, 100 mM NaCl, 1% NP-40, 1 mM DTT, and 2 mM PMSF) with protease inhibitor cocktail (Roche) in a 2-ml screw cap tube (Thermo Fisher Scientific). 2 g zirconia/silica 0.5-mm beads (Biospec Products, Inc.) were added and agitated for 3 min with a mini beadbeater (Biospec Products, Inc.) at 4°C. Lysates were cleared by centrifugation at 14,000 rpm for

Table 2. **The selected deletion strains expressing Sec15-3xGFP or co-expressing Sec4**

Strains	ORF
NY3002	MATa *his3Δ1 leu2Δ0 met15Δ0 ura3Δ0* Sec15-3xGFP::URA3
NY3003	MATa *his3Δ1 leu2Δ0 met15Δ0 ura3Δ0 apm4Δ::kanMX4* Sec15-3xGFP::URA3
NY3004	MATa *his3Δ1 leu2Δ0 met15Δ0 ura3Δ0 avl9Δ::kanMX4* Sec15-3xGFP::URA3
NY3005	MATa *his3Δ1 leu2Δ0 met15Δ0 ura3Δ0 chc1Δ::kanMX4* Sec15-3xGFP::URA3
NY3006	MATa *his3Δ1 leu2Δ0 met15Δ0 ura3Δ0 clc1Δ::kanMX4* Sec15-3xGFP::URA3
NY3007	MATa *his3Δ1 leu2Δ0 met15Δ0 ura3Δ0 swa2Δ::kanMX4* Sec15-3xGFP::URA3
NY3008	MATa *his3Δ1 leu2Δ0 met15Δ0 ura3Δ0 ccp1Δ::kanMX4* Sec15-3xGFP::URA3
NY3009	MATa *his3Δ1 leu2Δ0 met15Δ0 ura3Δ0 yap1802Δ::kanMX4* Sec15-3xGFP::URA3
NY3010	MATa *his3Δ1 leu2Δ0 met15Δ0 ura3Δ0 ldb17Δ::kanMX4* Sec15-3xGFP::URA3
NY3011	MATa *his3Δ1 leu2Δ0 met15Δ0 ura3Δ0* Sec15-3xGFP::URA3 Sec4::LEU2
NY3012	MATa *his3Δ1 leu2Δ0 met15Δ0 ura3Δ0 apm4Δ::kanMX4* Sec15-3xGFP::URA3 Sec4::LEU2
NY3013	MATa *his3Δ1 leu2Δ0 met15Δ0 ura3Δ0 avl9Δ::kanMX4* Sec15-3xGFP::URA3 Sec4::LEU2
NY3014	MATa *his3Δ1 leu2Δ0 met15Δ0 ura3Δ0 chc1Δ::kanMX4* Sec15-3xGFP::URA3 Sec4::LEU2
NY3015	MATa *his3Δ1 leu2Δ0 met15Δ0 ura3Δ0 clc1Δ::kanMX4* Sec15-3xGFP::URA3 Sec4::LEU2
NY3016	MATa *his3Δ1 leu2Δ0 met15Δ0 ura3Δ0 swa2Δ::kanMX4* Sec15-3xGFP::URA3 Sec4::LEU2
NY3017	MATa *his3Δ1 leu2Δ0 met15Δ0 ura3Δ0 ccp1Δ::kanMX4* Sec15-3xGFP::URA3 Sec4::LEU2
NY3018	MATa *his3Δ1 leu2Δ0 met15Δ0 ura3Δ0 yap1802Δ::kanMX4* Sec15-3xGFP::URA3 Sec4::LEU2
NY3019	MATa *his3Δ1 leu2Δ0 met15Δ0 ura3Δ0 ldb17Δ::kanMX4* Sec15-3xGFP::URA3 Sec4::LEU2

20 min and protein concentrations were determined using the Bio-Rad protein assay with BSA as a standard.

GST pull-down assays

GST-Snc2p pull-down of exocyst subunits. GST-Snc2p (purified from NRB1481, final concentration 0.2 µM) and yeast lysate (derived from NY2501, NY2502, NY2503, NY2504, NY2505, and NY2506, respectively, final concentration 2 µg/µl) were mixed in a total volume of 1 ml binding buffer (20 mM Pipes, pH 6.8, 100 mM NaCl, 1% NP-40, 1 mM DTT, and 2 mM PMSF) with protease inhibitor cocktail (Roche) and incubated on a rotator at 4°C for 2 h. Then 20 µl of a 50% suspension of glutathione beads was added and incubated at 4°C for another 2 h. The beads were washed four times with 1.4 ml binding buffer. The bound protein was analyzed by Western blot with anti-myc antibody (9E10). GST-Sec22p and GST-Sso2p were used as negative controls.

Determination of the dissociation constant (K_d) for Snc2p–Sec6p interaction. A quantitative GST pull-down assay (Pollard, 2010) was used to determine the K_d for Snc2p–Sec6p binding. In brief, GST-Snc2p (0–77 µM final concentration, purified from NRB1481) bound to glutathione beads was mixed with His-Sec6p (0.4 µM final concentration, purified from *E. coli*, NRB1485) in a total of 1 ml binding buffer and incubated on a rotator at 4°C for 2 h. The beads were pelleted by centrifugation at 5,000 rpm for 1 min and the supernatant protein was separated by SDS-PAGE and stained with Coomassie brilliant blue G250 (Bio-Rad Laboratories). The amount of Sec6p was quantified with ImageJ (National Institutes of Health) after scanning the gel and the K_d was calculated using Origin software (OriginLab Corporation).

Snc2p pull-down of Sec6p fragments. GST-Snc2p (0.05 µM final concentration, purified from NRB1481) and His-Sec6 fragments (0.05 µM final concentration, purified from NRB1474, NRB1475, NRB1476, NRB1477, NRB1478, and NRB1480) were mixed in 1 ml binding buffer and the pull-down was performed as described above. GST-Sec22p was used as a negative control.

Vamp3 pull-down of Exoc3. C-terminal Myc-tagged human Exoc3 was overexpressed by transfecting HeLa cells with a pCMV-Myc-Exoc3 plasmid (pNB1462). 36 µl FuGENE 6 transfection reagent (Promega) and 8 µg plasmid were used to transfect HeLa cells in 100-mm culture dishes at 80% confluence. The cells were harvested after 24 h, washed twice with 5 ml ice cold PBS, and lysed with 1 ml binding buffer (25 mM Hepes/KOH, pH 7.4, 150 mM NaCl, 1% NP-40, and 1 mM DTT, with protein inhibitor cocktail [Roche]). The lysate was cleared by centrifugation at 13,000 *g* for 15 min, mixed with bacteria lysates expressing GST (NRB1487), GST-Vamp4p (NRB1489), and GST-Vamp3p (NRB1488; 0.2 µM final concentration) and incubated at 4°C for 2 h. Glutathione beads (10 µl) were added and incubated for another hour. The beads were pelleted and washed three times with binding buffer before SDS-PAGE and Western blot analysis with anti-myc antibody.

Pull-down of Sec6p by Snc2p fragments or mutants. GST-Snc2p fragments (0.08 µM final concentration, purified from NRB1481, NRB1482, NRB1483, and NRB1484, respectively) or GST-Snc2p mutants (purified from NRB1462–1473, respectively) were used to perform pull-down assays with Sec6p (purified from NRB1485) as described above.

Competition assay of Snc2 and Sec9 for Sec6 binding. GST-Snc2p (from NRB1481) was bound to glutathione beads and purified. The beads were mixed with a constant amount of purified His-Sec6 (from NRB1485) and increasing amounts of His-MBP-Sec9ct (from NRB1486) in a total of 1 ml binding buffer (20 mM Pipes, pH 6.8, 100mM NaCl, 1% NP-40, 1 mM DTT, and 2 mM PMSF). The pull-down was performed as described above. Sec6p and Sec9ct pulled down by the beads were detected by Western blot using anti-His antibody (ABGENT).

Reconstitution and fusion

Proteoliposomes were produced as described previously (Scott et al., 2003). For t-SNARE liposomes, 250 µl of His_8-Sso1p (15 mg/ml) in 1% *n*-octyl-β-D-glucopyranoside (OG) and 250 µl GST-Sec9c (23 mg/ml) were mixed for ~15 h to form a t-SNARE complex and used to resuspend an acceptor lipid mix (POPC/DOPS [1-palmitoyl, 2-oleoyl phosphatidylcholine]/[1,2-dioleoyl phosphatidylserine], 85:15). For v-SNARE proteoliposomes, 50 µl of Snc2p-His_6 (1 mg/ml) or 100 µl of Snc2p-M2-His_6 (0.7 mg/ml) in 1% OG was used to resuspend a donor lipid mix (*N*-(7-nitro-2,1,3-benzoxadiazole-4-yl)-1,2-dipalmitoyl phosphatidylethanolamine [NBD-DPPE] and *N*-(lissamine rhodamine B sulfonyl) 1,2-dipalmitoyl phosphatidylethanolamine [Rhodamine-DPPE], 82:15:1.5:1.5) Proteoliposomes were formed by dilution and detergent removal achieved by flow dialysis overnight. Proteoliposomes were isolated by flotation in a discontinuous Nycodenz gradient. Protein content of the proteoliposomes was determined using an amido black protein assay (Schaffner and Weissmann, 1973) and lipid recovery determined by scintillation counting of trace tritiated 1,2-dipalmitoyl phosphatidlycholine added to the lipid mixes.

Fusion assays were also performed as described previously (Scott et al., 2003). 5 µl of labeled v-SNARE liposomes were mixed with 45 µl of unlabeled t-SNARE liposomes directly in a microtiter plate on ice. The plate was placed directly in the 37°C fluorescence plate reader (TECAN with Magellan software) without any prior preincubation.

Invertase assays

Invertase assays were adapted from the procedure described by Cai et al. (2005). In brief, cells were grown overnight at 25°C in YPD media (5% glucose) to early log phase (0.3–0.8 OD/ml). 1 OD of cells was pelleted, washed with 2 ml distilled water, and split into two equal aliquots and pelleted again. In one tube the cells were resuspended in 1 ml 10 mM NaN_3 and put on ice. In the other tube cells were resuspended in 1 ml YP 0.1% glucose and grown at 37°C with shaking for 1 h. Then the cells were pelleted, resuspended in 1 ml 10 mM NaN_3, and put on ice. For each sample, the external

Table 3. **Yeast strains used**

Strain	Genotype
NY17	Mat**a**, *ura3-52, sec6-4*
NY438	MATa *ura3 ade8 leu2 trp1 his3*
NY1745	MATα *ura3 ade8 leu2 tr1 his3*
NY1127	MATa *ura3 ade8 leu2 trp1 his3 snc1::URA3 snc2::ADE8* (2μ GAL1p-SNC1-HA-TRP1)
NY2977	MATa *ura3 ade8 leu2 trp1 his3* SEC6-2xmCherry::LEU2
NY2978	MATa *ura3 ade8 leu2 trp1 his3* SEC8-2xmCherry::LEU2
NY2979	MATα *ura3 ade8 leu2 tr1 his3* SEC15-3xGFP::HIS3
NY2980	MATa *ura3 ade8 leu2 trp1* his3 snc1::URA3 snc2::ADE8 (2μ GAL1p- SNC1-HA-TRP1) SEC6-2xmCherry::LEU2
NY2981	MATa *ura3 ade8 leu2 trp1 his3 snc1::URA3 snc2::ADE8* (2μ GAL1p- SNC1-HA-TRP1) SEC8-2xmCherry::LEU2
NY2982	MATa *ura3 ade8 leu2 trp1 his3 snc1::URA3 snc2::ADE8 (2μ GAL1p- SNC1-HA-TRP1) SEC15-3xGFP::HIS3*
NY2983	MATα his3Δ1 leu2Δ0 lys2Δ0 ura3Δ0 CHC1-mRFP1::kanMX6 SEC5-3xGFP::URA3
NY2984	MATα his3Δ1 leu2Δ0 lys2Δ0 ura3Δ0 CHC1-mRFP1::kanMX6 SEC15-3xGFP::URA3
NY2501	Mat**a** GAL+ *ura3-52 leu2-3,112 his3Δ200* SEC5::13myc(HIS3)
NY2502	Mat**a** GAL+ *ura3-52 leu2-3,112 his3Δ200* SEC6::13myc(HIS3)
NY2503	Mat**a** GAL+ *ura3-52 leu2-3,112 his3Δ200* SEC8::13myc(HIS3)
NY2504	Mat**a** GAL+ *ura3-52 leu2-3,112 his3Δ200* SEC10::13myc(HIS3)
NY2505	Mat**a** GAL+ *ura3-52 leu2-3,112 his3Δ200* SEC15::13myc(HIS3)
NY2506	Mat**a** GAL+ *ura3-52 leu2-3,112 his3Δ200* EXO70::13myc(HIS3)
NY2507	Mat**a** GAL+ *ura3-52 leu2-3,112 his3Δ200* EXO84::13myc(HIS3)
NY2985	MATa his3Δ1 leu2Δ0 met15Δ0 ura3Δ0 snc1Δ::kanMX4
NY2986	MATa *his3Δ1 leu2Δ0 met15Δ0 ura3Δ0 snc1Δ::kanMX4* SEC6-GFP::URA3
NY2987	MATa *his3Δ1 leu2Δ0 met15Δ0 ura3Δ0 snc1Δ::kanMX4* SEC15-3GFP::HIS3
NY2988	MATa *his3Δ1 leu2Δ0 met15Δ0 ura3Δ0 snc1Δ::kanMX4 snc2-M2(75E79E82E)*
NY2989	MATa *his3Δ1 leu2Δ0 met15Δ0 ura3Δ0 snc1Δ::kanMX4 snc2-M2(75E79E82E)* SEC6-GFP::URA3
NY2990	MATa *his3Δ1 leu2Δ0 met15Δ0 ura3Δ0 snc1Δ::kanMX4 snc2-M2(75E79E82E)* SEC15-3GFP::HIS3
NY2991	MATa *his3Δ1 leu2Δ0 met15Δ0 ura3Δ0 snc1Δ::kanMX4 snc2-V39A,M42A* SEC6-GFP::URA3
NY2992	MATa *his3Δ1 leu2Δ0 met15Δ0 ura3Δ0 snc1Δ::kanMX4 snc2-V39A,M42A* SEC15-3GFP::HIS3
NY2993	MATa *his3Δ1 leu2Δ0 met15Δ0 ura3Δ0 yap1801::his5 yap1802::kanMX4* SEC15-3xGFP::URA3
NY2994	MATa *his3Δ1 leu2Δ0 met15Δ0 ura3Δ0 avl9::kanMX4* GFP-SNC1::URA3
NY2995	MATa *his3Δ1 leu2Δ0 met15Δ0 ura3Δ0 chc1::kanMX4* GFP-SNC1::URA3
NY2996	MATa *his3Δ1 leu2Δ0 met15Δ0 ura3Δ0 clc1::kanMX4* GFP-SNC1::URA3
NY2997	MATa *his3Δ1 leu2Δ0 met15Δ0 ura3Δ0 swa2::kanMX4* GFP-SNC1::URA3
NY2998	MATa *his3Δ1 leu2Δ0 met15Δ0 ura3Δ0 ccp1::kanMX4* GFP-SNC1::URA3
NY2999	MATa *his3Δ1 leu2Δ0 met15Δ0 ura3Δ0 yap1802::kanMX4* GFP-SNC1::URA3
NY3000	MATa *his3Δ1 leu2Δ0 met15Δ0 ura3Δ0 yap1801::HIS5 yap1802::kanMX4* GFP-SNC1::URA3
NY3001	MATa *his3Δ1 leu2Δ0 met15Δ0 ura3Δ0 ldb17::kanMX4* GFP-SNC1::URA3

invertase was measured directly. The internal invertase was measured after cells were converted to spheroplasts and lysed in 0.5% Triton X-100.

Electron microscopy

Yeast cells of the *snc1Δ snc2-M2* mutant (NY2988) and *snc1Δ SNC2* (NY2985) control strains were grown at 25°C in YPD medium and processed for electron microscopy as described by Chen et al. (2012). Cells were fixed in 0.1 M cacodylate, 4% glutaraldehyde, pH 6.8, and the cell walls were enzymatically removed. The cells were then treated with 2% OsO_4 and then 2% uranyl acetate before dehydration in ethanol and embedding in Spurr resin. Sections were stained with lead citrate and UrAc. Images were acquired using a G2 Spirit transmission electron microscope (Tecnai) equipped with a CCD (charge-coupled device) camera (Ultra Scan 4000; Gatan, Inc.).

Table 4. **Plasmids for yeast transformation or HeLa cell transfection**

Name	Plasmid
pNB300	YCp50, GAL1-Sec15
PNB882	pRS306 SEC6-GFP
pNB1304	pRS306 SEC5-3xGFP
pNB1308	pRS306 SEC15-3xGFP
pNB1456	YCp50 GAL1-SEC15-GFP; a fragment of Sec15-GFP into BamH I–SalI sites of pNB300
pNB1457	pRS425 Sec4, a 392-bp Sec4 fragment was ligated into BamHI–XhoI sites
pNB1458	pRS303 Sec15-3xGFP; inserting Sec15-3xGFP-ADHterm fragment into pRS303 SalI–SacI sites
pNB1459	pRS305 Sec6-2xmCherry; inserted 1.6 kB Sec6 C-terminal fragment into XhoI–XbaI sites of pJC1-2xmCherry
pNB1460	pRS305 Sec8-2xmCherry; inserted 1 kB Sec8 C-terminal fragment into XhoI–XbaI sites of pJC1-2xmCherry
pNB1461	pRS306 Snc2-*M2(75E79E82E)*
pNB 1462	pCMV-myc-Exoc3
pSFNB1223	pRS416 GFP-SNC1

Table 5. **Bacterial strains used**

Strain	Plasmid	Host Strain
NRB1462	pAT110-snc2-R75A,R79A,K82A(M1); inserted into BamHI–XhoI sites of pAT110;kan^r	Rosetta
NRB1463	pAT110-snc2-R75E,R79E,K82E(M2); inserted into BamHI–XhoI sites of pAT110;kan^r	Rosetta
NRB1464	pAT110-snc2-E60A,D61A,D64A(M3); inserted into BamHI–XhoI sites of pAT110;kan^r	Rosetta
NRB1465	pAT110-snc2-E60K,D61R,D64R(M4); inserted into BamHI–XhoI sites of pAT110;kan^r	Rosetta
NRB1466	pAT110-snc2-E51A,E54A(M5); inserted into BamHI–XhoI sites of pAT110;kan^r	Rosetta
NRB1467	pAT110-snc2-E51R,E54R(M6); inserted into BamHI–XhoI sites of pAT110;kan^r	Rosetta
NRB1468	pAT110-snc2-R75A; inserted into BamHI–XhoI sites of pAT110;kan^r	Rosetta
NRB1469	pAT110-snc2-R75E; inserted into BamHI–XhoI sites of pAT110;kan^r	Rosetta
NRB1470	pAT110-snc2-R79A; inserted into BamHI–XhoI sites of pAT110;kan^r	Rosetta
NRB1471	pAT110-snc2-R79E; inserted into BamHI–XhoI sites of pAT110;kan^r	Rosetta
NRB1472	pAT110-snc2-K82A; inserted into BamHI–XhoI sites of pAT110;kan^r	Rosetta
NRB1473	pAT110-snc2-K82E; inserted into BamHI–XhoI sites of pAT110;kan^r	Rosetta
NRB1474	pQlink-His-TEV-Sec6 (1–805 aa); Amp^r	Rosetta
NRB1475	pQlink-His-TEV-Sec6 (292–805 aa); Amp^r	Rosetta
NRB1476	pQlink-His-TEV-Sec6 (411–805 aa); Amp^r	Rosetta
NRB1477	pQlink-His-TEV-Sec6 (1–411 aa); pCDF-GST-PreScission-Sec8(1–236 aa); Strep^r,Amp^r	Rosetta
NRB1478	pQlink-His-TEV-Sec6 (1–292 aa); pCDF-GST-PreScission-Sec8(1–236 aa); Strep^r,Amp^r	Rosetta
NRB1480	pCDF-GST-PreScission-Sec6(100–805 aa); Strep^r	Rosetta
NRB1481	pAT110-SNC2 (1–92 aa); inserted into BamHI–XhoI sites of pAT110;kan^r	Rosetta
NRB1482	pAT110-SNC2 (28–92 aa); inserted into BamHI–XhoI sites of pAT110;kan^r	Rosetta
NRB1483	pAT110-SNC2 (1–52 aa); inserted into BamHI–EcoRI sites of pAT110;kan^r	Rosetta
NRB1484	pAT110-SNC2 (53–92 aa); inserted into BamHI–XhoI sites of pAT110;kan^r	Rosetta
NRB1485	pET46-Sec6;Amp^r	Rosetta
NRB1486	pSV282-Sec9CT (416–651 aa); inserted into BamHI–EcoRI sites of pSV282;kan^r	Rosetta
NRB1487	pAT110;kan^r	Rosetta
NRB1488	pAT110-Vamp3; human Vamp3 cDNA inserted into BamH1–EcoR1 sites of pAT110 kan^r	Rosetta
NRB1489	pAT110-Vamp4; human Vamp4 cDNA inserted into the BamH1–Xho1 sites of pAT110 kan^r	Rosetta

Online supplemental material

Fig. S1 shows wild-type and mutant strains expressing GFP-Snc1p, imaged by fluorescence microscopy. Fig. S2 shows binding of His-tagged Sec6p, Exo70p, and Exo84p to beads carrying GST, GST-Sec22p, GST-Ykt6p, GST-Snc2p, GST-Sso1p, GST-Sso2p, or GST-Nyv1p. Fig. S3 shows binding of His-tagged Sec6p to beads carrying GST or GST-Snc1p. Fig. S4 shows binding of His-tagged Sec6p to GST-Sec22p, GST-Snc2p wild type, or to the indicated GST-Snc2p mutants. Online supplemental material is available at http://www.jcb.org/cgi/content/full/jcb.201211148/DC1. Additional data are available in the JCB DataViewer at http://dx.doi.org/10.1083/jcb.201211148.dv.

We thank Y. Jones in the Electron Microscopy Facility in the Department of Cellular and Molecular Medicine at the University of California at San Diego, headed by M. Farquhar, for the preparation of samples for electron microscopy. We also thank E. O'Shea for the Chc1p-RFP strain.

This work was supported by grants from the National Institutes of Health (GM35370 and GM082861 to P. Novick and GM071832 to J.A. McNew).

Submitted: 27 November 2012
Accepted: 1 July 2013

References

Boyd, C., T. Hughes, M. Pypaert, and P. Novick. 2004. Vesicles carry most exocyst subunits to exocytic sites marked by the remaining two subunits, Sec3p and Exo70p. *J. Cell Biol.* 167:889–901. http://dx.doi.org/10.1083/jcb.200408124

Burston, H.E., L. Maldonado-Báez, M. Davey, B. Montpetit, C. Schluter, B. Wendland, and E. Conibear. 2009. Regulators of yeast endocytosis identified by systematic quantitative analysis. *J. Cell Biol.* 185:1097–1110. http://dx.doi.org/10.1083/jcb.200811116

Cai, H., Y. Zhang, M. Pypaert, L. Walker, and S. Ferro-Novick. 2005. Mutants in trs120 disrupt traffic from the early endosome to the late Golgi. *J. Cell Biol.* 171:823–833. http://dx.doi.org/10.1083/jcb.200505145

Carr, C.M., and J. Rizo. 2010. At the junction of SNARE and SM protein function. *Curr. Opin. Cell Biol.* 22:488–495. http://dx.doi.org/10.1016/j.ceb.2010.04.006

Chen, S., P. Novick, and S. Ferro-Novick. 2012. ER network formation requires a balance of the dynamin-like GTPase Sey1p and the Lunapark family member Lnp1p. *Nat. Cell Biol.* 14:707–716. http://dx.doi.org/10.1038/ncb2523

Dong, G., A.H. Hutagalung, C. Fu, P. Novick, and K.M. Reinisch. 2005. The structures of exocyst subunit Exo70p and the Exo84p C-terminal domains reveal a common motif. *Nat. Struct. Mol. Biol.* 12:1094–1100. http://dx.doi.org/10.1038/nsmb1017

Fasshauer, D., R.B. Sutton, A.T. Brunger, and R. Jahn. 1998. Conserved structural features of the synaptic fusion complex: SNARE proteins reclassified as Q- and R-SNAREs. *Proc. Natl. Acad. Sci. USA*. 95:15781–15786. http://dx.doi.org/10.1073/pnas.95.26.15781

Ferro-Novick, S., and R. Jahn. 1994. Vesicle fusion from yeast to man. *Nature*. 370:191–193. http://dx.doi.org/10.1038/370191a0

Fölsch, H., M. Pypaert, S. Maday, L. Pelletier, and I. Mellman. 2003. The AP-1A and AP-1B clathrin adaptor complexes define biochemically and functionally distinct membrane domains. *J. Cell Biol.* 163:351–362. http://dx.doi.org/10.1083/jcb.200309020

Gall, W.E., M.A. Higginbotham, C. Chen, M.F. Ingram, D.M. Cyr, and T.R. Graham. 2000. The auxilin-like phosphoprotein Swa2p is required for clathrin function in yeast. *Curr. Biol.* 10:1349–1358.

Gall, W.E., N.C. Geething, Z. Hua, M.F. Ingram, K. Liu, S.I. Chen, and T.R. Graham. 2002. Drs2p-dependent formation of exocytic clathrin-coated vesicles in vivo. *Curr. Biol.* 12:1623–1627.

Grote, E., C.M. Carr, and P.J. Novick. 2000a. Ordering the final events in yeast exocytosis. *J. Cell Biol.* 151:439–452. http://dx.doi.org/10.1083/jcb.151.2.439

Grote, E., G. Vlacich, M. Pypaert, and P.J. Novick. 2000b. A snc1 endocytosis mutant: phenotypic analysis and suppression by overproduction of dihydrosphingosine phosphate lyase. *Mol. Biol. Cell*. 11:4051–4065. http://dx.doi.org/10.1091/mbc.11.12.4051

Guo, W., A. Grant, and P. Novick. 1999a. Exo84p is an exocyst protein essential for secretion. *J. Biol. Chem.* 274:23558–23564. http://dx.doi.org/10.1074/jbc.274.33.23558

Guo, W., D. Roth, C. Walch-Solimena, and P. Novick. 1999b. The exocyst is an effector for Sec4p, targeting secretory vesicles to sites of exocytosis. *EMBO J.* 18:1071–1080. http://dx.doi.org/10.1093/emboj/18.4.1071

Guo, W., F. Tamanoi, and P. Novick. 2001. Spatial regulation of the exocyst complex by Rho1 GTPase. *Nat. Cell Biol.* 3:353–360. http://dx.doi.org/10.1038/35070029

Gurkan, C., A.V. Koulov, and W.E. Balch. 2007. An evolutionary perspective on eukaryotic membrane trafficking. *Adv. Exp. Med. Biol.* 607:73–83. http://dx.doi.org/10.1007/978-0-387-74021-8_6

Harsay, E., and R. Schekman. 2007. Avl9p, a member of a novel protein superfamily, functions in the late secretory pathway. *Mol. Biol. Cell*. 18:1203–1219. http://dx.doi.org/10.1091/mbc.E06-11-1035

He, B., F. Xi, X. Zhang, J. Zhang, and W. Guo. 2007. Exo70 interacts with phospholipids and mediates the targeting of the exocyst to the plasma membrane. *EMBO J.* 26:4053–4065. http://dx.doi.org/10.1038/sj.emboj.7601834

Huh, W.K., J.V. Falvo, L.C. Gerke, A.S. Carroll, R.W. Howson, J.S. Weissman, and E.K. O'Shea. 2003. Global analysis of protein localization in budding yeast. *Nature*. 425:686–691. http://dx.doi.org/10.1038/nature02026

Hutagalung, A.H., J. Coleman, M. Pypaert, and P.J. Novick. 2009. An internal domain of Exo70p is required for actin-independent localization and mediates assembly of specific exocyst components. *Mol. Biol. Cell*. 20:153–163. http://dx.doi.org/10.1091/mbc.E08-02-0157

Katz, L., P.I. Hanson, J.E. Heuser, and P. Brennwald. 1998. Genetic and morphological analyses reveal a critical interaction between the C-termini of two SNARE proteins and a parallel four helical arrangement for the exocytic SNARE complex. *EMBO J.* 17:6200–6209. http://dx.doi.org/10.1093/emboj/17.21.6200

Kloepper, T.H., C.N. Kienle, and D. Fasshauer. 2008. SNAREing the basis of multicellularity: consequences of protein family expansion during evolution. *Mol. Biol. Evol.* 25:2055–2068. http://dx.doi.org/10.1093/molbev/msn151

Lewis, M.J., B.J. Nichols, C. Prescianotto-Baschong, H. Riezman, and H.R. Pelham. 2000. Specific retrieval of the exocytic SNARE Snc1p from early yeast endosomes. *Mol. Biol. Cell*. 11:23–38. http://dx.doi.org/10.1091/mbc.11.1.23

Maldonado-Báez, L., M.R. Dores, E.M. Perkins, T.G. Drivas, L. Hicke, and B. Wendland. 2008. Interaction between Epsin/Yap180 adaptors and the scaffolds Ede1/Pan1 is required for endocytosis. *Mol. Biol. Cell*. 19:2936–2948. http://dx.doi.org/10.1091/mbc.E07-10-1019

McNew, J.A., F. Parlati, R. Fukuda, R.J. Johnston, K. Paz, F. Paumet, T.H. Söllner, and J.E. Rothman. 2000. Compartmental specificity of cellular membrane fusion encoded in SNARE proteins. *Nature*. 407:153–159. http://dx.doi.org/10.1038/35025000

McNiven, M.A., and H.M. Thompson. 2006. Vesicle formation at the plasma membrane and trans-Golgi network: the same but different. *Science*. 313:1591–1594. http://dx.doi.org/10.1126/science.1118133

Mizuno-Yamasaki, E., F. Rivera-Molina, and P. Novick. 2012. GTPase networks in membrane traffic. *Annu. Rev. Biochem.* 81:637–659. http://dx.doi.org/10.1146/annurev-biochem-052810-093700

Morgera, F., M.R. Sallah, M.L. Dubuke, P. Gandhi, D.N. Brewer, C.M. Carr, and M. Munson. 2012. Regulation of exocytosis by the exocyst subunit Sec6 and the SM protein Sec1. *Mol. Biol. Cell*. 23:337–346. http://dx.doi.org/10.1091/mbc.E11-08-0670

Munson, M., and P. Novick. 2006. The exocyst defrocked, a framework of rods revealed. *Nat. Struct. Mol. Biol.* 13:577–581. http://dx.doi.org/10.1038/nsmb1097

Novick, P., and P. Brennwald. 1993. Friends and family: the role of the Rab GTPases in vesicular traffic. *Cell*. 75:597–601. http://dx.doi.org/10.1016/0092-8674(93)90478-9

Novick, P., and W. Guo. 2002. Ras family therapy: Rab, Rho and Ral talk to the exocyst. *Trends Cell Biol.* 12:247–249. http://dx.doi.org/10.1016/S0962-8924(02)02293-6

Novick, P., C. Field, and R. Schekman. 1980. Identification of 23 complementation groups required for post-translational events in the yeast secretory pathway. *Cell*. 21:205–215. http://dx.doi.org/10.1016/0092-8674(80)90128-2

Pishvaee, B., G. Costaguta, B.G. Yeung, S. Ryazantsev, T. Greener, L.E. Greene, E. Eisenberg, J.M. McCaffery, and G.S. Payne. 2000. A yeast DNA J protein required for uncoating of clathrin-coated vesicles in vivo. *Nat. Cell Biol.* 2:958–963. http://dx.doi.org/10.1038/35046619

Pollard, T.D. 2010. A guide to simple and informative binding assays. *Mol. Biol. Cell*. 21:4061–4067. http://dx.doi.org/10.1091/mbc.E10-08-0683

Protopopov, V., B. Govindan, P. Novick, and J.E. Gerst. 1993. Homologs of the synaptobrevin/VAMP family of synaptic vesicle proteins function on the late secretory pathway in *S. cerevisiae*. *Cell*. 74:855–861. http://dx.doi.org/10.1016/0092-8674(93)90465-3

Salminen, A., and P.J. Novick. 1989. The Sec15 protein responds to the function of the GTP binding protein, Sec4, to control vesicular traffic in yeast. *J. Cell Biol.* 109:1023–1036. http://dx.doi.org/10.1083/jcb.109.3.1023

Schaffner, W., and C. Weissmann. 1973. A rapid, sensitive, and specific method for the determination of protein in dilute solution. *Anal. Biochem.* 56:502–514. http://dx.doi.org/10.1016/0003-2697(73)90217-0

Scott, S.V., D.C. Nice III, J.J. Nau, L.S. Weisman, Y. Kamada, I. Keizer-Gunnink, T. Funakoshi, M. Veenhuis, Y. Ohsumi, and D.J. Klionsky. 2000. Apg13p and Vac8p are part of a complex of phosphoproteins that are required for cytoplasm to vacuole targeting. *J. Biol. Chem.* 275:25840–25849. http://dx.doi.org/10.1074/jbc.M002813200

Scott, B.L., J.S. Van Komen, S. Liu, T. Weber, T.J. Melia, and J.A. McNew. 2003. Liposome fusion assay to monitor intracellular membrane fusion machines. *Methods Enzymol.* 372:274–300. http://dx.doi.org/10.1016/S0076-6879(03)72016-3

Sivaram, M.V., J.A. Saporita, M.L. Furgason, A.J. Boettcher, and M. Munson. 2005. Dimerization of the exocyst protein Sec6p and its interaction with the t-SNARE Sec9p. *Biochemistry*. 44:6302–6311. http://dx.doi.org/10.1021/bi048008z

Sommer, B., A. Oprins, C. Rabouille, and S. Munro. 2005. The exocyst component Sec5 is present on endocytic vesicles in the oocyte of Drosophila melanogaster. *J. Cell Biol.* 169:953–963. http://dx.doi.org/10.1083/jcb.200411053

Strop, P., S.E. Kaiser, M. Vrljic, and A.T. Brunger. 2008. The structure of the yeast plasma membrane SNARE complex reveals destabilizing water-filled cavities. *J. Biol. Chem.* 283:1113–1119. http://dx.doi.org/10.1074/jbc.M707912200

Sutton, R.B., D. Fasshauer, R. Jahn, and A.T. Brunger. 1998. Crystal structure of a SNARE complex involved in synaptic exocytosis at 2.4 A resolution. *Nature*. 395:347–353. http://dx.doi.org/10.1038/26412

TerBush, D.R., T. Maurice, D. Roth, and P. Novick. 1996. The Exocyst is a multiprotein complex required for exocytosis in *Saccharomyces cerevisiae*. *EMBO J.* 15:6483–6494.

Whyte, J.R., and S. Munro. 2001. The Sec34/35 Golgi transport complex is related to the exocyst, defining a family of complexes involved in multiple steps of membrane traffic. *Dev. Cell*. 1:527–537. http://dx.doi.org/10.1016/S1534-5807(01)00063-6

Yu, I.M., and F.M. Hughson. 2010. Tethering factors as organizers of intracellular vesicular traffic. *Annu. Rev. Cell Dev. Biol.* 26:137–156. http://dx.doi.org/10.1146/annurev.cellbio.042308.113327